REPORT DOCUMENTATION PAGE

Form Approved
OMB No. 0704-0188

1. REPORT DATE *(DD-MM-YYYY)*	**2. REPORT TYPE**	**3. DATES COVERED** *(From - To)*
August 2013	Technical Paper	August 2013- September 2013

4. TITLE AND SUBTITLE
Background Pressure Effects on Krypton Hall Effect Thruster Internal Acceleration

5a. CONTRACT NUMBER
In-House

5b. GRANT NUMBER

5c. PROGRAM ELEMENT NUMBER

6. AUTHOR(S)
William A. Hargus, Jr., Landon J. Tango, Michael R. Nakles

5d. PROJECT NUMBER

5e. TASK NUMBER

5f. WORK UNIT NUMBER
Q09W

7. PERFORMING ORGANIZATION NAME(S) AND ADDRESS(ES)

Air Force Research Laboratory (AFMC)
AFRL/RQRS
1 Ara Drive.
Edwards AFB CA 93524-7013

8. PERFORMING ORGANIZATION REPORT NO.

9. SPONSORING / MONITORING AGENCY NAME(S) AND ADDRESS(ES)
Air Force Research Laboratory (AFMC)
AFRL/RQR
5 Pollux Drive
Edwards AFB CA 93524-7048

10. SPONSOR/MONITOR'S ACRONYM(S)

11. SPONSOR/MONITOR'S REPORT NUMBER(S)
AFRL-RQ-ED-TP-2013-226

12. DISTRIBUTION / AVAILABILITY STATEMENT
Distribution A: Approved for Public Release; Distribution Unlimited. PA#13488

13. SUPPLEMENTARY NOTES
Conference paper for the International Electric Propulsion Conference 2013, Washington, D.C., 6-10 October 2013.

14. ABSTRACT
This study uses krypton propellant in a medium power Hall effect to amplify the effect of background pressure due to the greater mobility of neutral krypton compared to neutral xenon. The use of krypton amplifies the effect of elevated background pressures by enhancing the population of neutrals capable of reaching into the critical ionization and acceleration regions within a Hall effect thruster discharge. As ground test facilities cannot reach pressures comparable to those in LEO or GEO, these measurements provide a useful benchmark for determining the effects and methods to mitigate the inherent limitations of available ground test facilities as well as providing data for comparison to future simulations and experiments. Using the 728.98 nm 5*d*4 *D*7/2–5*p*4 *P* ◦ Kr II transition, we successfully measured ion velocities via laser–induced fluorescence in the near–plume and within the acceleration channel of a laboratory model, medium power Hall effect thruster. With these measurements and historical data, we are able to estimate the neutral number density from neutral velocity and propellant utilization estimates for both xenon and krypton operation. From these measurements and calculations, we show that the relative number density of the neutrals in the acceleration channel compared to the background neutral number density at the thruster exit appears to be an important parameter to determining the degree to which the thruster is sensitive to background pressure.

15. SUBJECT TERMS

16. SECURITY CLASSIFICATION OF:			**17. LIMITATION OF ABSTRACT**	**18. NUMBER OF PAGES**	**19a. NAME OF RESPONSIBLE PERSON**
					William Hargus
a. REPORT	**b. ABSTRACT**	**c. THIS PAGE**	SAR	32	**19b. TELEPHONE NO** *(include area code)*
Unclassified	**Unclassified**	**Unclassified**			661-525-6799

Background Pressure Effects on Krypton Hall Effect Thruster Internal Acceleration

William A. Hargus, Jr.*
Landon J. Tango†
Michael R. Nakles‡
Air Force Research Laboratory, Edwards Air Force Base, CA 93524

This study uses krypton propellant in a medium power Hall effect to amplify the effect of background pressure due to the greater mobility of neutral krypton compared to neutral xenon. The use of krypton amplifies the effect of elevated background pressures by enhancing the population of neutrals capable of reaching into the critical ionization and acceleration regions within a Hall effect thruster discharge. As ground test facilities cannot reach pressures comparable to those in LEO or GEO, these measurements provide a useful benchmark for determining the effects and methods to mitigate the inherent limitations of available ground test facilities as well as providing data for comparison to future simulations and experiments. Using the 728.98 nm $5d^4\,D_{7/2}$–$5p^4\,P^{\circ}_{5/2}$ Kr II transition, we successfully measured ion velocities via laser–induced fluorescence in the near–plume and within the acceleration channel of a laboratory model, medium power Hall effect thruster. With these measurements and historical data, we are able to estimate the neutral number density from neutral velocity and propellant utilization estimates for both xenon and krypton operation. From these measurements and calculations, we show that the relative number density of the neutrals in the acceleration channel compared to the background neutral number density at the thruster exit appears to be an important parameter to determining the degree to which the thruster is sensitive to background pressure.

Introduction

Understanding the effects of ground test facility background pressure on Hall effect thrusters has become a critical interest to the spacecraft propulsion community. Models and limited test data have shown significant changes occur in the regions of acceleration both within and in the near plume of Hall effect thrusters. Previous measurements have examined the changes in the acceleration regions of a medium power (600 W) xenon Hall effect thruster between 3.1×10^{-5} Torr and 1.2×10^{-5} Torr and found substantial differences in the acceleration profiles. These differences have been attributed to differences in periodic plasma fluctuations that are believed to strongly affect internal electron mobility.[1] As these pressure ranges have traditionally been viewed as sufficient for both short and long term testing of Hall effect thrusters,[2] there is now an impetus to better characterize the limitations of ground test facilities and determine how they may be mitigated.

While xenon is in many ways the ideal propellant for electrostatic thrusters such as Hall effect thrusters, there are a number of supply concerns that have driven the Hall effect thruster community to explore alternative propellants. Due to the low concentration of xenon in the atmosphere (~90 ppb), worldwide production is only approximately 6,000 standard cubic meters per year. Increasing industrial demand for items such as high efficiency lighting and windows, as well as plasma based micro-fabrication, has produced wide price swings in the past decade. Krypton is approximately 10× more common in the atmosphere (and hence in production) than xenon, and when accounting for mass is approximately 6× less expensive. For missions that can benefit from higher specific impulse, krypton may have benefits beyond its lower cost. Krypton has a lower atomic mass (83.8 amu), but a slightly higher ionization potential (14.0 eV) than xenon. Like xenon, krypton is a noble gas and could be easily integrated into existing Hall effect thruster propellant management systems without much modification. Similar ionization potential should not dramatically affect Hall effect thruster efficiency, and the lower atomic mass of krypton could produce a 25% increase in specific impulse. Table 1 summarizes relevant properties of xenon and krypton.[3]

A substantial body of simulation and experimental knowledge has determined that the optimization of Hall effect thrusters for krypton versus xenon demand that the thruster geometry be specialized based on propellant choice. Several researchers have theorized and verified that krypton performance can approach the performance estimated from parametric extrapolation from xenon optimized thrusters.[4,5,6,7] These previous studies have demonstrated that relative to xenon

*Senior Engineer, AFRL/RQRS, Edwards AFB, CA, USA.
†Engineer, ERC, Inc., Edwards AFB, CA, USA
‡Senior Engineer, ERC, Inc., Edwards AFB, CA, USA

Hall effect thrusters, krypton Hall effect thrusters require longer ionization regions and higher magnetic fields producing higher electron temperatures to produce comparable propellant utilization (i.e. propellant flow ionization fraction). Without optimization, krypton does not appear to be simple *drop-in replacement* for xenon for existing thrusters optimized for xenon.[7]

The examination of krypton propellant in otherwise unmodified thrusters with substantial xenon heritage also provides an avenue for the fundamental study of Hall effect thruster discharge physics since ideally the only operational changes are due to the ion/neutral mass and electron–impact ionization cross–sections as shown in Table 1.

This study uses krypton propellant in a medium power Hall effect to amplify the effect of background pressure due to the greater mobility of neutral krypton compared to neutral xenon as kryptons sonic velocity is 125% that of xenon. The use of krypton amplifies the effect of elevated background pressures by enhancing the population of neutrals that reach into the critical ionization and acceleration regions within a Hall effect thruster. Similar to previous work with xenon propellant in the same thruster,[1] we examine a minimum facility pressure (1.2×10^{-5} Torr) and an elevated, but still deemed acceptable for long duration testing,[2] facility pressure of 3.2×10^{-5} Torr. Our method for non–intrusively probing the krypton discharge is laser induced fluorescence of the Kr II metastable population recently developed at our laboratory[8] to measure the ion velocity distributions and characterize changes with background pressure. Previous work on xenon,[1] showed that substantial changes in the velocity distributions occurred due to differences in the dynamical behavior of the xenon plasma in response to background pressure. As ground test facilities cannot reach pressures comparable to those in LEO or GEO, these measurements provide a useful benchmark for determining the effects and methods to neutralize the inherent limitations of available test facilities, as well as providing data for comparison for numerical simulations.

Laser-Induced Fluorescence

Laser-induced fluorescence (LIF) may be used to detect velocity–induced shifts in the spectral absorption of various plasma species. The fluorescence is monitored as a continuous-wave laser is tuned in frequency over the transition of interest, of energy $h\nu_{12}$, where h is Plank's constant, ν_{12} is wavenumber of transition between lower state 1 and higher energy state 2. Note that state 1 may be the ground state, but any sufficiently highly populated excited state will do. In this work, we have chosen to examine a metastable state to ensure higher signal levels. Measurements can be made with high spatial resolution, determined by the intersection of the probe laser beam with the fluorescence optical collection volume.

Table 1 Comparison of xenon and krypton properties critical for electrostatic propulsion.[3]

Property	Units	Xe	Kr
Atomic Mass	amu	131.3	83.8
1^{st} Ionization Energy	eV	12.1	14.0
2^{nd} Ionization Energy	eV	21	24
3^{rd} Ionization Energy	eV	32	37
Atmospheric Concentration	ppb	87	1000
Stable Isotopes		9	6
Odd Isotopes		2	1
Critical Pressure	MPa	5.84	5.50
Critical Temperature	K	290	209
Boiling Point (1 atm)	K	161	120

Velocity measurements may be made using LIF velocimetry as an atom, or as in our case an ion, moving with a velocity component u relative to the direction of the incoming laser will absorb photons at a frequency shifted from that of stationary absorbers due to the Doppler effect. The magnitude of this frequency shift $\delta\nu_{12}$ is

$$\delta\nu_{12} = \frac{u}{c}\nu_{12}. \tag{1}$$

The measured fluorescence lineshape is determined by the environment of the absorbing ion population, so an accurate measurement of the lineshape function may lead to the determination of a number of plasma parameters beyond simple bulk velocities. The precision of measured velocities has been found, in various studies, to be less than the experimental uncertainty (±500 m/s)[9, 10, 11]

LIF is a convenient diagnostic for the investigation of ion velocities in a plasma thruster as it does not physically perturb the discharge. The LIF signal is a convolution of the velocity distribution function (VDF), transition lineshape, and laser beam frequency profile. Determination of the VDF from LIF data only requires the deconvolution of the transition lineshape and laser beam profile from the raw LIF signal trace. Alternatively, the lineshape itself may also provide valuable information on the state of the plasma, such as electron density, pressure, or heavy species temperature. In the somewhat turbulent plasmas typical of Hall effect thrusters, the fluorescence lineshape can also be indicative of the relative motion of the ionization zone as it axially traverses in the periodic breathing mode plasma fluctuation.[12, 13] However, care must be taken to ensure that the relative effects of these phenomena are separable. In addition, magnetic (Zeeman effect) and electric (Stark effect) fields may also influence the fluorescence lineshape[14] and must be accounted for when analyzing the lineshapes should the fields be of sufficient magnitude. In the case of LIF of ions in a Hall effect thruster, the fluorescence lineshape

appears to be most indicative of the aforementioned plasma turbulence including periodicity in the positions of the ionization zone within the acceleration channel.

The Kr II $5d^4D_{7/2}$–$5p^4P^\circ_{5/2}$ transition at 728.98 nm emanating from the metastable $5d^4D_{7/2}$ state provides a highly populated excited state ion population that is easily accessible via diode laser spectroscopy. This transition has been studied and developed for laser-induced fluorescence by ourselves and others studying the acceleration dynamics of krypton Hall effect thrusters.[15, 16, 17, 8] The details of application of LIF using the metastable $5d^4D_{7/2}$ state and exciting to the $5p^4P^\circ_{5/2}$ state using a laser at 728.98 nm are detailed elsewhere.[8]

Apparatus

Vacuum Facility and Thruster

The LIF measurements were performed in Chamber 6 of the Air Force Research Laboratory (AFRL) Electric Propulsion Laboratory at Edwards AFB, CA. Chamber 6 is a non-magnetic stainless steel chamber with a 1.8 m diameter and 3 m length. Pumping is provided by four single–stage cryogenic panels (single–stage cold heads at 25 K) and one 50 cm two stage cryogenic pump (12 K). This vacuum test chamber has a measured maximum pumping speed of approximately 36,000 L/s on xenon and krypton.

The Hall thruster used in this study is a medium power laboratory Hall effect thruster, which has been described elsewhere.[1] This thruster is designed for operation on xenon and performance is not optimized for krypton, although extensive plume measurements are available.[18] Thruster operation for this effort consisted of a single stable condition shown on Table 2. Unpublished thrust measurements from our laboratory show krypton operation of the BHT-600 at the conditions in Table 2 yields a thrust of 22.4 mN corresponding to an anode efficiency of approximately 31%. Also, during thruster operation, the thruster operational parameters shown in Table 2 are monitored and recorded at a 0.2 Hz data rate.

Chamber pressure during thruster operation is monitored with a cold cathode ionization gauge located behind the thruster. The cold cathode gauge is located external to the chamber on a 25 mm diameter tube approximately 100 mm in length, behind a 0.5 mm mesh screen mounted on the chamber wall. During low pressure operation, the chamber background pressure is measured to be 1.2×10^{-5} Torr (nitrogen calibrated cold cathode gauge with a reading of 2.0×10^{-5} Torr corrected for krypton using N_2 conversion to Kr multiplicative factor of 0.59[19]). High pressure operation is achieved via injection of 40 sccm of krypton at a location above the thruster with a krypton corrected background pressure determined to be 3.1×10^{-5} (N_2 calibrated reading of 5.2×10^{-5} Torr). Figure 1 shows a diagram with the relative positions of thruster, cold cathode pressure gauge, krypton inlet, and cryogenic pump panels. For the purposes of clarity, that the LIF launch and collection optics are not shown in Fig. 1.

Table 2 ***Nominal thruster operating conditions.***

Kr Anode Flow	25.5 sccm (1.59 mg/s)
Kr Cathode Flow	1.5 sccm (94 μg/s)
Anode Potential	300 V
Anode Current	1.73 A
Inner Coil Current	4.0 A
Outer Coil Current	4.0 A
Keeper Current	0.5 A
Heater Current	3.0 A
Thrust	22.4 mN
Anode Efficiency	31%
Specific Impulse	1440 s

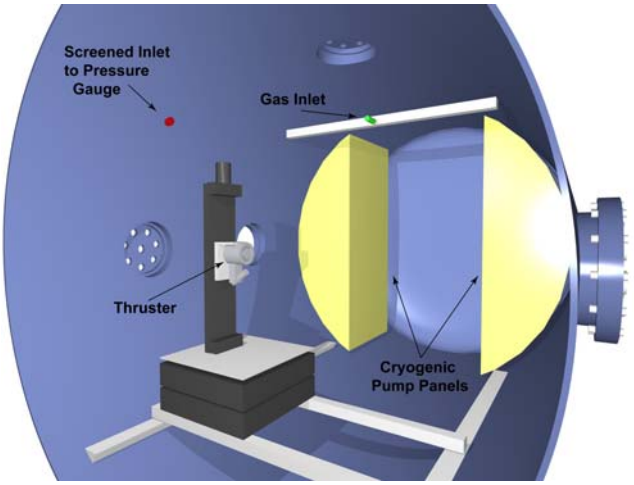

Fig. 1 Scale diagram showing the thruster location, location of screened inlet to cold cathode pressure gauge, additional krypton injection point, and cryogenic pumping panels. For clarity, the optics for launch and collection of the laser-induced fluorescence are not shown.

Laser and Optics

The laser used in this study is a custom built ±50 GHz tunable diode laser (Newport Optics, New Focus Division) centered on the $5d^4D_{7/2}$–$5p^4P^\circ_{5/2}$ transition with a maximum of 25 mW output power. This laser is a Littman–Metcalf external cavity tunable diode laser capable of mode hop free tuning across approximately 100 GHz tuning range at output powers as high as 25 mW with a line width of less than 500 kHz.

Based on previous efforts,[20, 8] the laser, probe beam launch optics, and fluorescence collection optics are located on two optical tables placed about viewports with optical access into the vacuum chamber as shown in Fig. 2. On the primary optics table, the diode

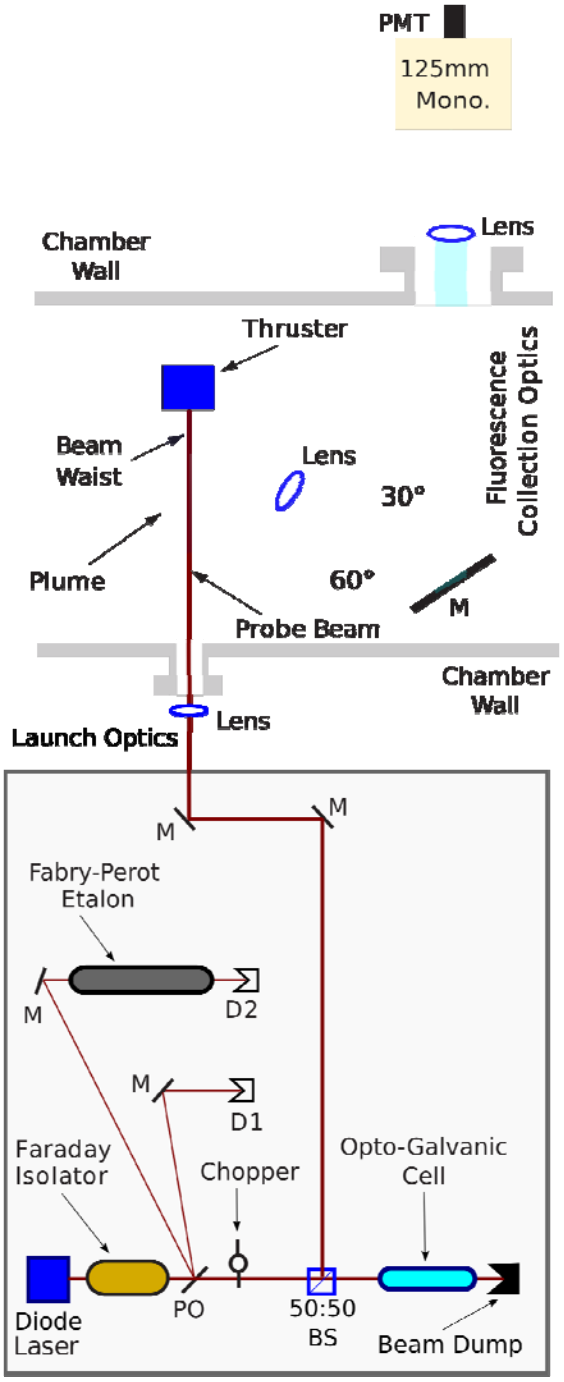

Fig. 2 Layout of Kr II laser-induced fluorescence apparatus showing all relevant optical components, portions of the vacuum chamber, and Hall effect thruster thruster plume.

laser beam first passes through a Faraday isolator to eliminate laser feedback. The laser beam then passes through a 10% wedged beam pick–off (PO) to provide beam diagnostics. The first of the two reflections (each approximately 5% of incident power) is directed onto a photodiode detector (D1) and provides constant power feedback to the laser. The second pick–off beam passes through a 300 MHz free spectral range, high finesse Fabry–Perot etalon (F–P) that provides frequency monitoring of the wavelength interval swept during a laser scan.

The main laser beam is then chopped at 3 kHz by a mechanical optical chopper for phase sensitive detection. It is then divided into two equal components by a 50:50 cube beam splitter (BS). The first component passes through a krypton opto-galvanic cell and is terminated by a beam dump. The opto-galvanic cell current is capacitively coupled to a lock-in amplifier in order to monitor the Kr II 728.98 nm $5d^4D_{7/2}$–$5p^4P^\circ_{5/2}$ transition to provide a zero velocity reference.[21]

The probe beam is then directed via several mirrors and focused by a single lens to a sub-millimeter beam waist within the chamber vacuum through a glass vacuum viewport. The fluorescence collection optics also shown in Fig. 2 collect the signal generated at the beam waist. The fluorescence is collected by a 75 mm diameter, 300 mm focal length lens within the chamber. The collimated signal is directed through a window in the chamber side wall to a similar lens that focuses the collected fluorescence onto the entrance slit of 125 mm focal length monochrometer with a photomultiplier tube (PMT) detector. The PMT signal is then analyzed using a second lock-in amplifier. The spatial resolution of the measurements is determined by the geometry of the spectrometer entrance slit (note the 1:1 magnification of the collection optics). For these measurements, the measurement volume is approximately 500 μm diameter by 1 mm length.

Measurement Domain

Figure 3 shows a cross-section of the BHT-600 Hall effect thruster used in this test. Annotated in red is the measurement volume. The volume consists of a linear set of data points spaced by 2 mm at X=0, Y=28 mm with Z varying between -8 mm and +12 mm. This measurement set overlaps the measurements of Nakles and Hargus who measured the xenon acceleration in the same region of the same thruster at similar conditions.[1]

Krypton Velocity Measurements and Analysis

As previously stated, raw fluorescence traces are a reasonable representation of the Kr ion velocity distribution (VDF). Recall that the fluorescence traces are the convolution of the true VDF, the transition line shape, and the laser line width. The transition lineshape has been modeled and found to be relatively narrow compared to the fluorescence trace.[15, 16] In turn, the laser line width is only approximately 500 kHz wide. As a result, the fluorescence line shape magnitude is within 10–15% of the time averaged VDF, and generally better except for the sharpest features. This is consistent with previous velocity distribution measurements for xenon that showed that deconvolu-

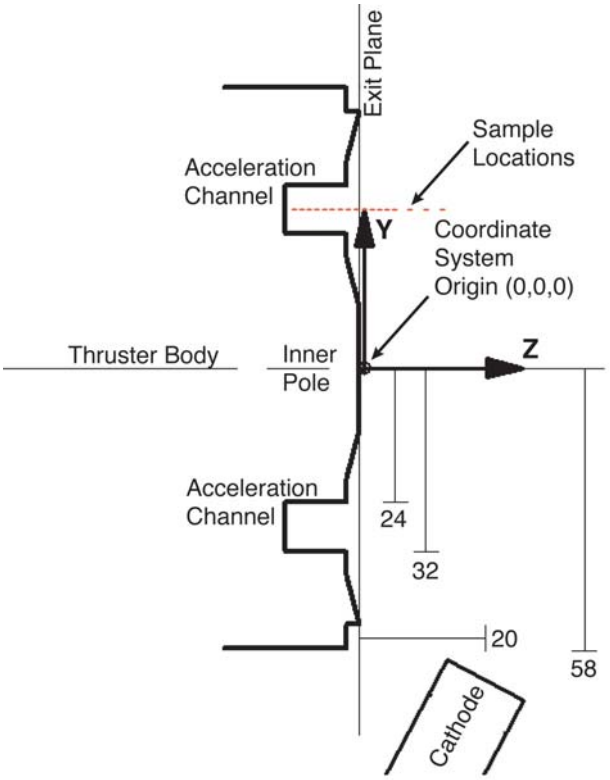

Fig. 3 Cutaway view of the BHT-600 Hall effect thruster with measurement volume shown in red. All dimensions are given in mm.

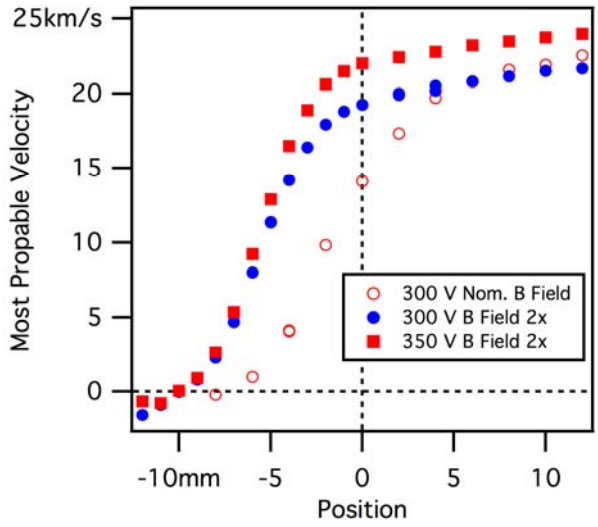

Fig. 4 Most probable axial Kr II velocities for three cases. Open circles represent nominal conditions from previous measurements.[23] Filled circles are for nominal conditions with 2× applied magnetic field Filled squares are likewise with an increased applied discharge potential (350 V vs. 300 V nominal).

tion of the transition lineshape was not necessary in the near plume to extract adequate approximations to the velocity distribution.[22]

Effect of Thruster Discharge Parameters

While a number of others have examined krypton as a Hall effect thruster propellant theoretically and experimentally, the number of ion velocity measurements is very limited. Many of the original Kr II LIF measurements measured the ionized propellant acceleration in thrusters with conditions very similar, or identical, to xenon operational parameters.[8, 16, 17, 23] These studies have utility due to their ability to directly compare the plasma acceleration between propellants with similar control parameters. However, it has been observed that optimum krypton Hall effect thruster performance requires at a minimum the optimization of the discharge parameters and ideally optimization of the thruster geometry.[7]

In our study, we are not able to optimize the thruster geometry due to equipment constraints. We have been able to increase the magnetic field strength by a factor of two (×2), and increase the discharge potential by approximately 15%. These modifications of the thruster operational parameters by no means optimize krypton thruster performance, but are anticipated to increase electron temperature, thereby increasing propellant utilization producing better performance. Ideally, we would have increased the discharge potential by a factor of two (×2) over the nominal 300 V xenon typical operational value, but our apparatus was constrained due to 350 V allowing for some margin on the anode power supplies that could not exceed 400 V.

Figure 4 shows the *most probable velocity* of the krypton ions velocity distributions measured via LIF. The most probable velocity represents the peak of the velocity distribution. This value is easily discerned with minimum ambiguity from both clean and noisy data. The most probable velocity should not be considered to be representative of the mean nor median values as relatively broad, non-symmetrical velocity distributions occur, especially near the exit plane.

From Fig. 4, we see that differences between the low and high magnetic field cases produce substantial changes in the ion velocity profiles. The 300 V discharge potential data at nominal magnetic (B) field was previously presented.[23] Similar to xenon, increases of the magnetic field in the krypton case push the ion acceleration inward toward the anode.

The effect of magnetic field on the effective electric field calculated by squaring and differentiation of the most probable velocity data show some similarities, as well as some differences as characterized in Fig. 5. In the xenon case, take from previously published data,[1, 13] the electric field peak is pushed into the thruster channel by increases in the magnetic field. The shift is small, only approximately 2 mm, but measurable. The effective electric field decreases some, but only approximately 10%. Comparing nominal mag-

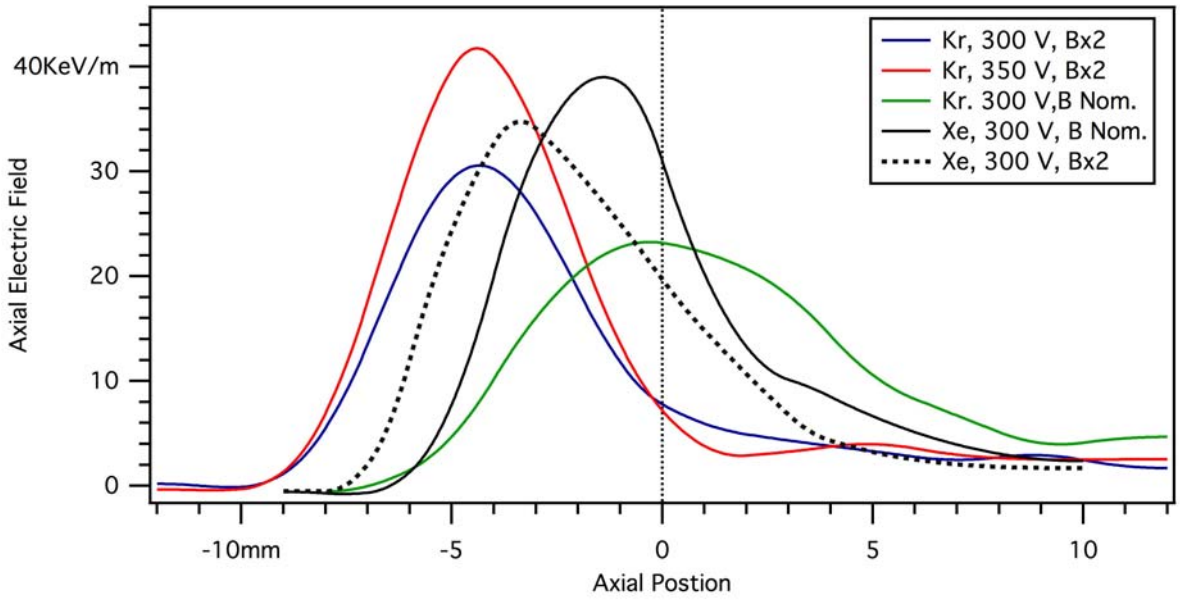

Fig. 5 Effective electric fields calculated from most probable velocity profiles for xenon, krypton at various operating condition. The nominal krypton magnetic field (B Nominal) electric field data[23] and xenon electric field data[1,13] are from previous publications.

netic field strength krypton[23] results to higher applied magnetic field cases produced in this study, also shifts the peak electric field into the thruster channel. However, for krypton, the shift is approximately 5 mm, and instead of a small decrease in the effective electric field we see a 20% increase in the electric field at an applied discharge potential of 300 V.

The increases in the magnetic field and discharge potential raised to 350 V produce conditions substantially closer to that characterized for xenon at nominal conditions. This is consistent with recent discussions as to the utility of xenon optimized Hall effect thrusters with krypton propellant. Bugrova et al.[7] convincingly show that substantial increases in electron temperature, plasma density, and channel length are necessary for krypton to match and potentially improve on the performance of xenon state of the art Hall effect thrusters. The key differences between xenon and krypton optimization is the slightly higher ionization energy of krypton (14 eV versus 12.1 eV for xenon) and the higher sonic velocity (125%). These effects jointly reduce ionization probability unless the aforementioned plasma parameters are adjusted for krypton relative to xenon.

We recognize that the present operating conditions are not yet optimized for krypton. The goal of this study is not to optimize the krypton conditions, but rather to contrast the fundamental differences between the two propellants in a carefully controlled experiment. Here we isolate the propellant as the only experimental control variable and focus on the observed differences. Figure 5 shows that we have substantial differences in the various cases examined; however, the effective electric fields also show that the cases at elevated magnetic field (denoted in this work as $B \times 2$) are similar in their general behavior, much more so than the case previously compared in our previous study.[23] This is due to more typical peak electric field located within the thruster channel. We acknowledge, that optimum krypton operation requires further work and exploration for this thruster. However, this study is valuable as a basis of comparison between propellants. We feel that it provides fundamental insights of the critical processes under investigation and separates them based on differences attributable to propellant atomic mass and ionization potential. In this study, the effect of atomic mass difference and ionization potentials allows us to change new variables to gain understanding of the effects of facility background pressure on thruster operation.

Variation of Chamber Background Pressure

For the measurements in this study, two vacuum chamber background pressure operating conditions were operated. The first referred to as *low pressure* operation was the equilibrium pressure maintained by the facility during thruster operation. This condition is measured to be 1.2×10^{-5} Torr (nitrogen calibrated cold cathode gauge with a reading of 2.0×10^{-5} Torr corrected for krypton using N_2 conversion to Kr multiplicative factor of 0.59[19]).

The second operating condition, referred in this work as the *high pressure* operation is achieved via injection of 50 sccm of krypton at a location above the thruster with a krypton corrected background pressure determined to be 3.1×10^{-5} (N_2 calibrated reading of 5.2×10^{-5} Torr). For completeness, Fig. 1 in the apparatus portion of the manuscript shows a diagram with

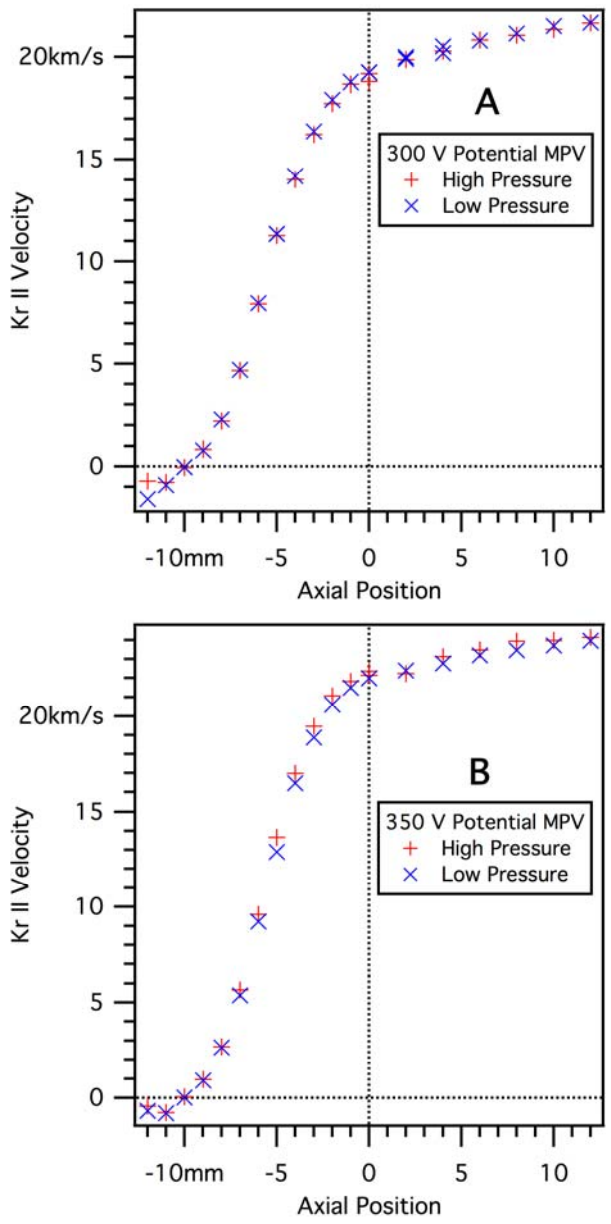

Fig. 6 Comparisons of most probable velocities, MPV, for 300 V (A) and 350 V (B) applied acceleration potentials.

the relative positions of thruster, cold cathode pressure gauge, krypton inlet, and cryogenic pump panels.

Figure 6 compares the most probable velocities of the measured Kr II ion axial velocity distributions for both 300 V and 350 V acceleration potentials. The effect of increasing the background pressure appears to be minimal for the krypton cases. At 300 V acceleration potential there is no substantial change in the most probable velocities from point to point as the repeatability of the measurement is within ±200 m/s. The difference at $Z = -12$ mm is believed to be due to low signal and the appearance of the multiple velocity distribution peaks. At 350 V acceleration potential, increasing krypton facility pressure appears produces a systematic increase in the interior velocities that may be as high as 1 km/s, but the differences are relatively small. The resultant effective electric field is moved toward the anode consistent with the previous xenon measurements, but to a lesser degree.

A more comprehensive methodology to interpret these data and the differences due to the background pressure on the acceleration of the krypton ions is to look at the velocity distributions. With regard to the velocity distributions, we assume that the extracted fluorescence traces are functionally equivalent to the velocity distributions. Previous studies that sought to deconvolve the lineshape have shown that unless the fluorescence peaks are particularly narrow, deconvolving the transition lineshape has a negligible effect.[22]

Figures 7 and 8 contain the velocity distributions based on the LIF fluorescence traces. As was noted in Fig. 4, the peaks of the distributions are not significantly affected by the increase in the background pressure during thruster operation as such the most probable velocities do not change significantly. Figures 7 and 8 show that the effect is more subtle. Velocity distributions at higher background pressure are broader. We attribute this increase in breadth of the velocity distribution to changes in the oscillatory behavior of the plasma driven by the change of the ambient conditions. Some these unsteady behavior also manifest themselves as more signal noise on the LIF traces with increasing background pressure.

Both the 300 V and 350 V cases demonstrate similar behavior. Both cases exhibit velocity distribution broadening, especially near the exit plane, as the background pressure increases. In addition, neither case shows a substantial change in the effective energy deposition or hence the effective electric field as did previous xenon testing at similar pressures.[1] However, there also appear some curious differences in the data. The broadening of the 300 V case near the thruster geometrical exit is much greater than that of the 350 V case. Although the 350 V case shows some shifting in the primary acceleration region of the distribution peaks (i.e. most probable velocities), the broadening is not as severe as in the 300 V case.

Previous velocity distribution measurements for this thruster in xenon and krypton have shown a characteristic narrowing of the velocity distribution both near the anode and toward the exit plane, with the widest portion of the distribution in the central portion of the thruster discharge channel. This behavior is consistent with the overlap of the ionization and ion acceleration regions. It denotes the extent of that overlap. As the neutrals available for ionization are depleted, kinematic compression of the velocity distribution occurs and the net effect is a narrower overall velocity spread. The difference between the 300 V and 350 V cases where the breadth of the velocity distributions

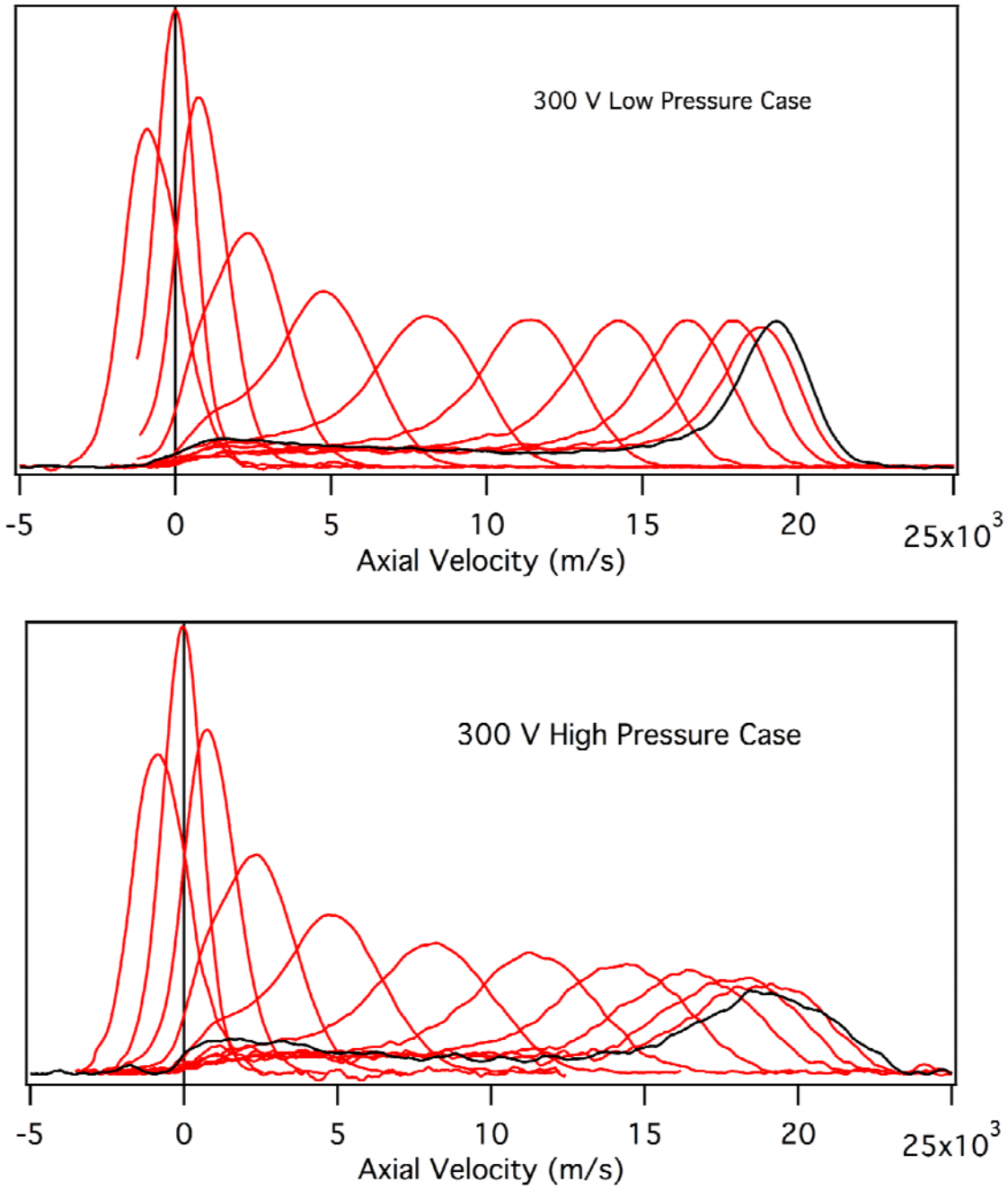

Fig. 7 Krypton ion (Kr II) velocity distributions for 300 V discharge potential at low background pressure (upper) and high background pressure (lower) ranging from the thruster exit plane (black trace at $Z = 0$ mm) to $Z = -11$ mm near the anode.

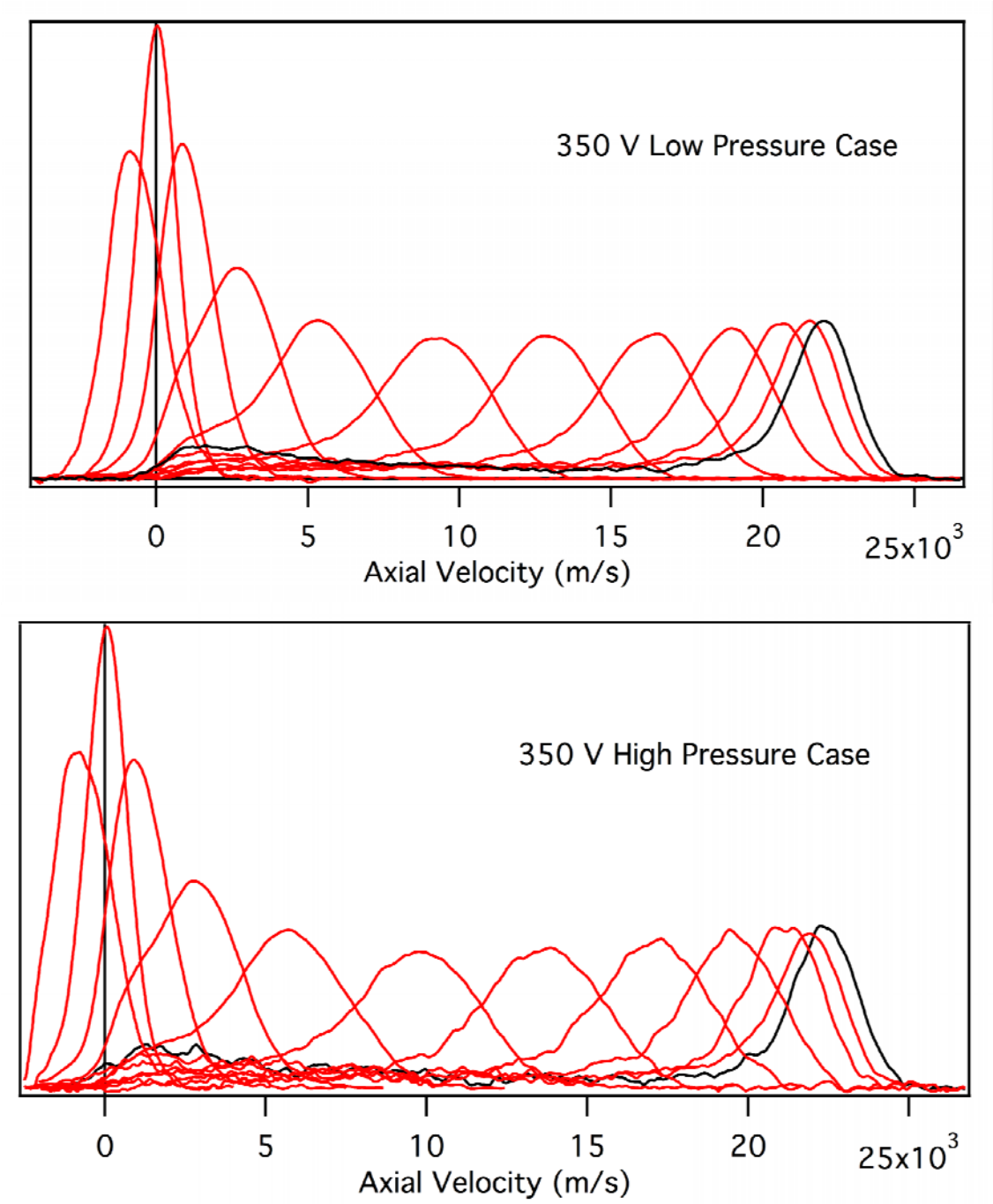

Fig. 8 Krypton ion (Kr II) velocity distributions for 350 V discharge potential at low background pressure (upper) and high background pressure (lower) ranging from the thruster exit plane (black trace at $Z = 0$ mm) to $Z = -11$ mm near the anode.

has such different behavior is therefore surprising. Although not shown in Figs. 7 and 8, in all data sets, external acceleration produces a substantial narrowing of the velocity distribution. This was also previously seen for xenon.

Several interpretations of the continued velocity distribution broadening of the high pressure case of 300 V discharge potential can be made in the lower plot of Fig. 7. One possibility is that the ionization region continues external to the thruster geometry. This implies a new source of neutrals such as ingestion. This has been a concern at high operating conditions for some time and is commonly cited when attempting to determine what on-orbit performance might be based from ground test.[2] Alternatively, oscillations enhancing turbulent plasma transport may change the characteristic length of the ionization region first proposed by Fife.[24] The use of a characteristic ionization length has been used to describe the breathing mode frequency common to Hall effect thrusters as a periodic axial ionization wave.[25]

From the data gathered in this study it is difficult to narrow the source of these subtle changes in ion acceleration. Ingestion is supported by the higher populations of low velocity ions at the exit plane in the lower plots of Figs. 7 and 8 (note that the black traces denote velocity distributions at the exit plane in each data plot). Both the 300 V and 350 V cases exhibit this behavior and generation of more low energy ions implies local ionization. The increase in plasma oscillations is significantly more subtle, if it is indeed present. Oscillation magnitude in the discharge current increased slightly with both increased background chamber pressure and discharge potential. The effects were not perceived during testing to be significant as they did not produce substantial changes in the oscillation frequency. However, these changes require further examination in light of the results presented above.

Several of our previous studies[1, 13] focused on the differences in electron transport driven by the intrinsic plasma oscillations. It is hypothesized that plasma oscillations arise from discharge electron starvation requiring turbulent transport to enhance local electron mobility. Observations show that moderate increases in test chamber background pressure appear to move the acceleration region into the thruster relative to lower background pressures. We have attributed this behavior to increased electron mobility due to increased turbulent plasma transport, whereby stochastic azimuthal plasma density fluctuations facilitate $\boldsymbol{E} \times \boldsymbol{B}$ electron transport across the applied radial magnetic field lines thus sustaining the plasma discharge. The increased mobility produces an extension of the acceleration region thus resulting in a natural broadening of the distribution. However, as shown in Fig. 6, the most probable velocity is unchanged. One issue that may need to be addressed to resolve this quandary are time resolved studies of these behaviors as the mean behavior may not illustrate the degree of change that might be more evident on the μs time scale.

Analysis

From the data presented, the environment produced by the Hall effect thruster plasma discharge in conjunction with the test facility environment needs to be considered as a whole. In Fig. 9, we show a number of critical densities at the thruster exit and test chamber environment. The chamber background pressure is derived from the perfect gas law, $P = nkT$. The neutral density has not been adequately measured and must be derived from related measurements. We choose to estimate density based on limited existing neutral velocity data in the literature.[26, 9, 27] These data indicate that the velocity of the neutrals is in excess of sonic for ambient temperature (assumed to be 300 K for all calculations) due to depletion of the neutrals with longest residence. Hence, those neutrals with higher axial velocities are least likely to be ionized.

Propellant utilization is defined as the ratio of ion flux to total propellant input and can be estimated by examining integrated ion currents and thrust measurements of a Hall effect thruster.[28, 18, 29] From these measurements, we presume that an efficiently operated xenon Hall effect thruster operates with a propellant utilization fraction of approximately 0.90. From our performance measurement of krypton operation on the same thruster, the propellant fraction is substantially lower, approximately 80% of that of xenon, or 0.72. These propellant utilization fractions are noted on Fig. 9 as black vertical lines.

The most likely range of neutral velocities is estimated to be between 1× and 2× the room temperature sonic speed based on previous measurements. The derived neutral densities are plotted as a function of ionization fraction on Fig. 9 as a range based on 1× to 2× room temperature (300 K) sonic velocities. Exit plane ion velocities as a function of propellant utilization for both krypton and xenon are calculated using 20 km/s and 15 km/s speeds measured previously. All densities are calculated using the cross-sectional area of the BHT-600 thruster, and therefore are only strictly valid at thruster channel exit. Finally, shown in red are the background pressure limits, shown as densities at an assumed ambient temperature of 300 K. The background pressure of 5×10^{-5} Torr is prescribed by Randolph et al. as the maximum pressure of long duration testing.[2] While, the background chamber pressure of 1×10^{-5} Torr is from experience a more typical background pressure at which much Hall effect testing is performed. This range encompasses the background pressures for much Hall effect thruster testing, particularly for higher power Hall effect thrusters that are limited by available ground based facilities.

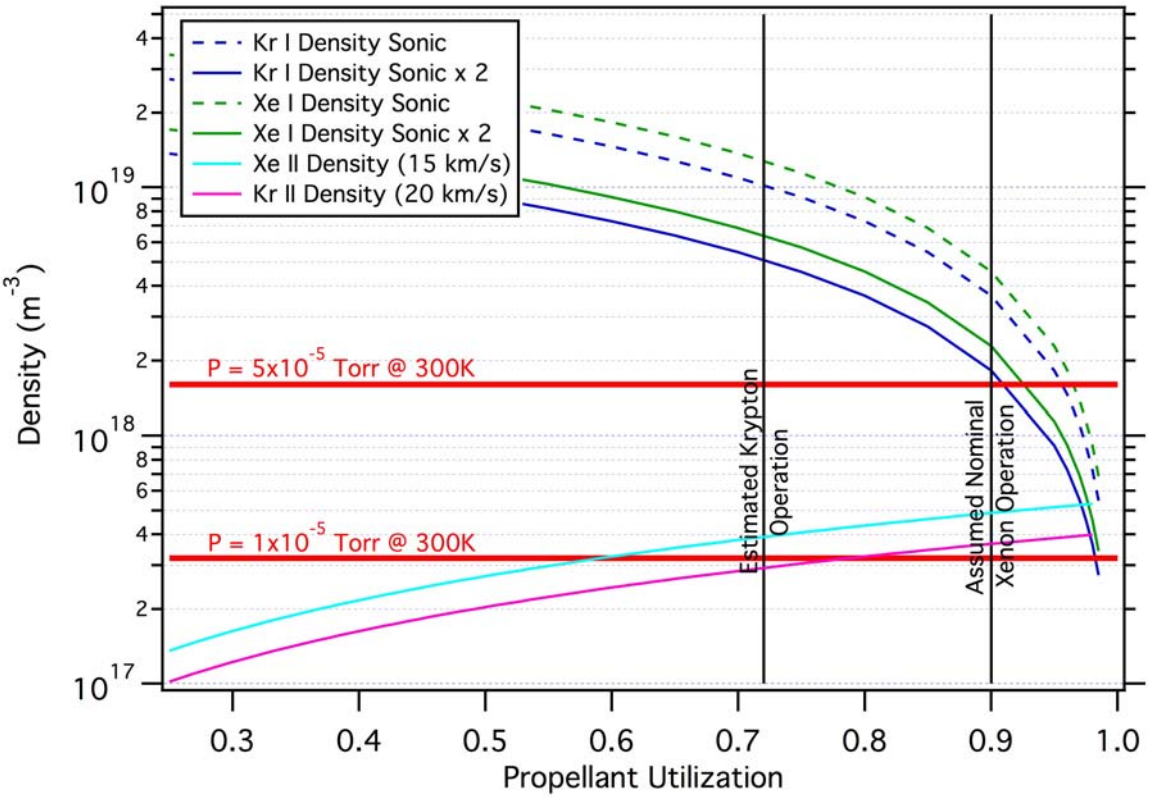

Fig. 9 Relevant exit plane densities of neutrals and ion calculated from velocity measurements for xenon and krypton cases examined. Also shown in red are the typical background densities for typical test chamber operational pressures.

Figure 9 immediately illustrates several non-intuitive facts about Hall effect thruster operation. First, even though 70% to 90% of the propellant is ionized prior to exiting the thruster, the disparate velocities of the neutrals and ions produce neutral densities that are between 5× and 10× higher than the ion densities. Second, the accepted upper limit of the high vacuum maintained by the test facilities is approximately that of the exit plane neutral density and 2× or 3× higher than the ion density. Furthermore, the lower acceptable background pressure of 1×10^{-5} Torr produces a background neutral density approximately equal to that of the ions. From Fig. 9, it must be recognized that the Hall effect thruster is a complex interplay of neutral and ion populations. Even at accepted high efficiency operation (e.g. 0.9 propellant utilization fraction), the exit plane of a Hall thruster is dominated by the neutral density.

The previous measurements on xenon propellant acceleration with this thruster with a similar variation in background pressure[1] can be illuminated using Fig. 9. The high pressure operation on xenon placed the background and exiting neutral densities at comparable magnitudes, both higher than the ion density. While the low pressure operation on xenon placed the background neutral density and the ion density at approximately equal magnitudes, both substantially lower than exiting neutral density. Notionally, the higher background neutral density would be expected to enhance classical electron mobility. However, increased background density increases discharge turbulence, presumably further enhancing transport as seen in that study.

The mechanism producing such a dramatic change in xenon Hall effect thruster operation is not clearly identified at this time. The introduction of background neutrals may result in downstream ionization events that change the local plasma properties (i.e. plasma density and hence the local plasma conductivity). If there is a competing neutral refresh mechanism from the test facility, it may interfere with the periodic ionization wave that governs the characteristic *breathing mode*.[25] If multiple neutral refresh events interfere with one another, it may explain the differences in operational behavior for xenon background pressure.[1] However, much remains speculative with respect to cause and effect at this time.

Surprisingly, no such parallel dramatic change in operational behavior occurs for the krypton case. Figure 9 provides possible insights into this apparent contradiction. With our estimate of low krypton propellant utilization, we see that the neutral density in the channel of non-ionized propellant is higher than either the low or high background pressure cases. The

background krypton neutral density is approximately equal or slightly higher than the exiting krypton ion density. While the data presented thus far does shown some changes in the breadth of the velocity Kr II distributions with increasing background density, we do not see a dramatic shift in the internal ion acceleration profile.

The obvious difference between the krypton and xenon cases is the higher density of the krypton neutrals exiting the thruster relative to the background neutral density. The neutral density due to the escaping thruster neutrals is approximately 6× to 10× that of the test chamber background neutrals at the thruster exit for either the higher and low background pressure cases, respectively. This implies that effect of the background neutrals is muted by the higher density exiting the thruster. Therefore, the low efficiency thruster operating on krypton does not experience the dramatic shift in performance previously seen in xenon operation since the low krypton propellant utilization provided a dominant source of neutrals.

However, there are still verifiable effects on ion acceleration for the krypton cases with increasing background neutral density. Figure 10 shows the ion energy distributions calculated from the velocity distributions in Fig. 8 for the 350 V discharge potential case of krypton. The integrated krypton ion distributions produce a graphical view of the ion acceleration. As presented the data present the graphical representation of the integration of the ion populations as a function of their energy at various axial locations within the thruster channel.

In Fig. 10 we see that deep within the thruster channel, the acceleration proceeds monotonically in that the curves of integrated population fraction show a steady increase in energy without overlapping previous locations that would indicate a local increase in the population of very slow ions, which indicates increases in local ionization. We see this behavior between the anode and $Z = -4$ mm.

For the high pressure case at $Z = -3$ mm, we see the integrated population overlap that of the $Z = -4$ mm population at approximately 0.06 ion population fraction. Therefore, we see that approximately 1% of the population at $Z = -3$ mm has an ion energy of less than 10 eV. At $Z = 0$, the exit plane, we see that approximately 3% of the ion population has an ion velocity of less than 10 eV. Similar behavior holds for the low pressure case.

The differences between the low and higher background pressure cases Fig. 10 are subtle. The high pressure case appears to have greater population fractions at very low ion energies, although the differences are relatively small. The higher pressure case also appears to have a higher population fraction at cross-over to a previous location's population. For the high background pressure case, it is as high as 0.20, where the low background pressure is more typically 0.13.

The overlaps in population shown in Fig. 10 indicate changes in the rate of late term ionization. So while Fig. 8 shows that late term ionization is occurring throughout the thruster channel, Fig. 10 shows that the rate of late term ionization increases significantly in the region between the exit plane and $Z = -4$ mm. While the changes in the energy distributions between the low and high background pressure cases are small, they are identifiable.

We then re-examined the xenon data from the previous xenon study[1] to determine if we could find similar behavior in the integrated energy distributions. These analyses of the 300 V data at high magnetic field are shown in Fig. 11. Here, we see correlating evidence that the high pressure xenon case bears similarities to that of the krypton case where we see an apparent increase in late term ionization in the high background pressure case. However upon examination and compilation of these data, we determined that the xenon data were considerably noisier than the krypton data. We have determined that the xenon data were taken with a 3× shorter averaging period that decreased the signal to noise ratio (SNR) by approximately 2×. This decrease in SNR was confirmed by analysis of the fluorescence signal background noise. We also observed that the xenon operation was substantially noisier than krypton, particularly in the region around the exit plane. As the thruster operation on xenon at high pressures was particularly rough, these effects were magnified for the critical higher background pressure case. As a result, the population fractions below 0.03 and those nearest the exit plane should be viewed cautiously. Those traces that exhibited the most uncertainty in their integration due to background noise are shown as dashed lines. This traces showed substantial background noise that we believe masked the behavior of population fractions of less than 0.1.

These comparisons to xenon data are illuminating. It appears that similar behavior to that shown in the krypton cases are evident in the Hall effect thruster channel. Due to the higher mass of xenon, one would expect the ingestion of xenon to be lower. This is implied by the limited available data. Ingestion appears to be occurring for high background pressure xenon case at $Z = -3$ mm where late term ionization is implied by the population of less than 40 eV ions. Interestingly, the low background pressure xenon data does not show this apparent ingestion. The noisy background of the xenon fluorescence data, especially nearest the exit plane precludes definitive conclusions, but the evidence appears consistent with this supposition.

It is interesting to consider methods used to reduce the background pressure. In Fig. 9, we assumed an ambient temperature of the background neutrals of 300 K. We note that some chambers are cryogenically

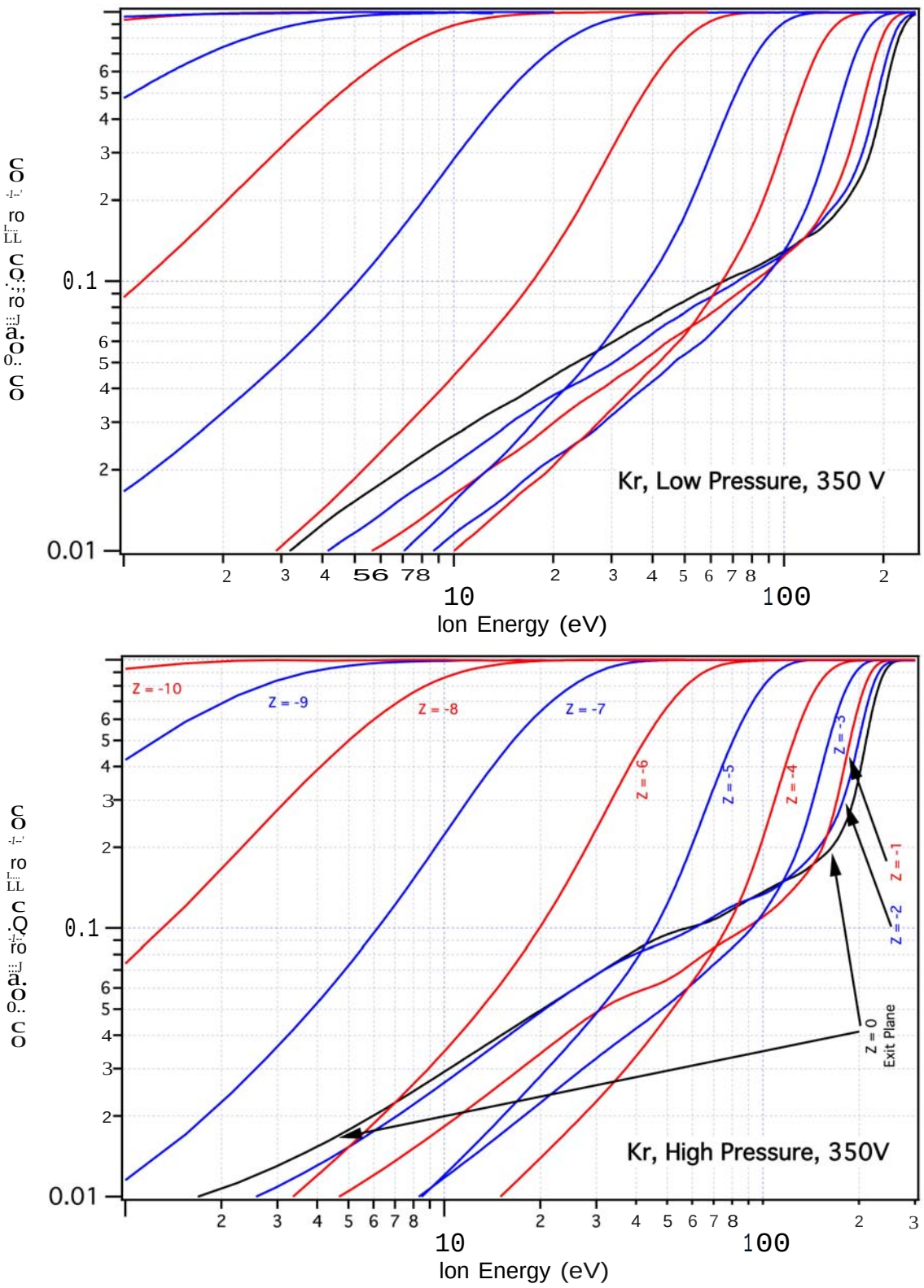

Fig. 10 Integrated krypton ion energy distributions calculated from krypton velocity distributions for the 350 V discharge potential case. The exit plane is denoted by the black line and subsequent axial locations are noted by their axial position. Note the apparent increase in late term ionization in the high background pressure case when compared to the lower pressure case.

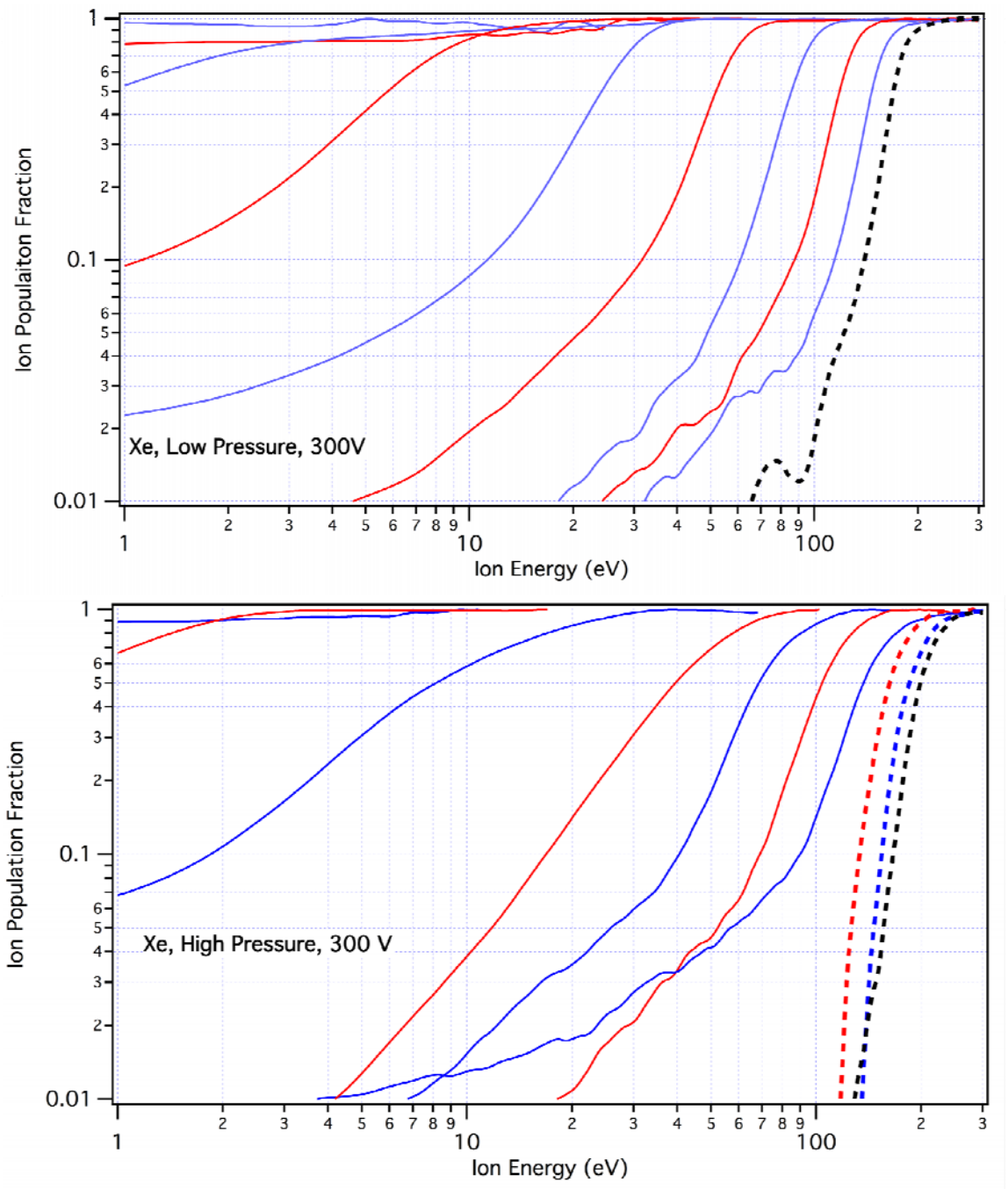

Fig. 11 Integrated xenon ion energy distributions calculated from xenon velocity distributions for the 300 V discharge potential case from Nakles and Hargus.[1] The exit plane is denoted by the black line and subsequent axial locations are noted by their axial position. Note the dashed lines are used to denote populations with greater than typical noise in the fluorescence signal that may have masked the behavior of population fractions of less than 0.1.

pumped and have very large liquid nitrogen arrays. Several such facilities exist at national test facilities such as those at NASA Glenn Research Center, or at the U.S. Air Force Arnold Engineering Center. If we take the pressure to be lowered by reducing the mean temperature of the background neutrals, via the ideal gas law, $P = nkT$ (where P is the pressure, T is the temperature, n is the number density, and k is Boltzmann's constant), then the density of the background neutrals may remain higher than anticipated despite the low pressure. As such $n \sim P/T$, and the density could be as much as $4\times$ higher (76 K vs 300 K). If the particle flux into the discharge or the near plume is the critical parameter, then the dependency becomes $\xi \sim P/T^{1/2}$, where ξ is the random particle flux across an arbitrary surface. As a result, it appears important to better characterize the neutral background density in these test chambers. If only 25% of the interior of a facility is cooled to liquid nitrogen temperatures (76 K), the background density n may be as much as $2\times$ higher than that assumed by pressure measurements and the use of ambient temperature. Similarly, the neutral flux ξ would be twice as high as anticipated. This simple analysis illustrates that care than needs to be placed on how the background density is calculated and evaluated.

Conclusions

This effort has sought to determine the ingestion behavior of krypton and compare it to xenon data from similar measurements. These results have produced evidence of a background pressure dependency for late term ionization inside the exit plane of a medium power Hall effect thruster operating on both xenon and krypton. As expected krypton showed a greater amount of late term ionization, believed to be due to the higher mobility of the lighter species enabling higher transport of neutrals into the discharge from the ambient environment of the chamber background.

However, the effect of increased vacuum facility background pressure did not produce as dramatic of a change in thruster operation in krypton as in xenon. We attribute this difference to the lower propellant utilization fraction of the krypton case. The resulting higher fraction of non–ionized propellant exiting the thruster appears to have increased the local neutral density to a level that relatively small increases in the background density do not have an appreciable effect. Previous measurements on the xenon thruster with a substantially higher propellant utilization demonstrated greater influence of the background pressure on the ion acceleration profile, and this is believed to be due to the background neutral density being higher than the density of non–ionized xenon neutrals exiting the thruster. An analysis of the pressures traditionally deemed acceptable for ground testing shows that these guidelines should be reconsidered based on these results.

The density of neutrals in the background of Hall effect ground test facilities appears to have measurable effects on thruster operation. Higher performing thrusters appear to have a greater susceptibility to facility background pressure due to their fuller utilization of propellant. In addition, we believe that facility background neutral density and temperature are as important of a facility characterization as the background pressure and should be considered when attempting to account for effects of testing in ground based facilities.

It is obvious that the effects of ground test facilities on Hall effect thruster operation on are not well understood on a fundamental basis. One reason for this present state of affairs is that there has been limited study into the various phenomena and that the focus of technology developers and integrators has been on mitigation, rather than fundamental understanding. We believe that the effects of ground test conditions should be divided in to three overlapping regions. These regions approximately correspond to the thruster discharge, mid–plume, and far–plume. Figure 12 shows graphically our proposed division of the critical regions of the Hall effect thruster discharge and plume. The discharge includes the region where the anode and cathode interact, including the the interior thruster channels and the near–plume region exterior to the thruster body to the vicinity of the cathode. The discharge region is denoted by the green box. The mid-plume region consists of the luminous plume, which appears to correspond to the region of the plume where collisional processes are relatively common. The mid–plume is located within the white box. The far–plume we define as the region of the plume where collisions are relatively uncommon and do not play a critical role in the plasma dynamics and in Fig. 12 it is the region outside the dashed yellow polygon.

In our proposed classification, the thruster discharge consists of the interior discharge starting at the anode where the bulk of ionization and propellant acceleration occurs. It would also include the near plume where a significant portion of the energy deposition and electron transport from the cathode to the anode occurs. Notionally this region consists of the region where ionization and ion acceleration occur both within and just outside of the thruster to the vicinity of the cathode. This region represents the plasma discharge of the thruster. Therefore, it is critical to understand the degree to which the test environment affects this region as the plasma is created in this region and must necessarily propagate from here.

We define the mid–plume region as that region where there exists a luminous plume outside of the thruster channel. This region overlaps with the near plume between the cathode and thruster physical exit. Measurements via LIF have shown that the central

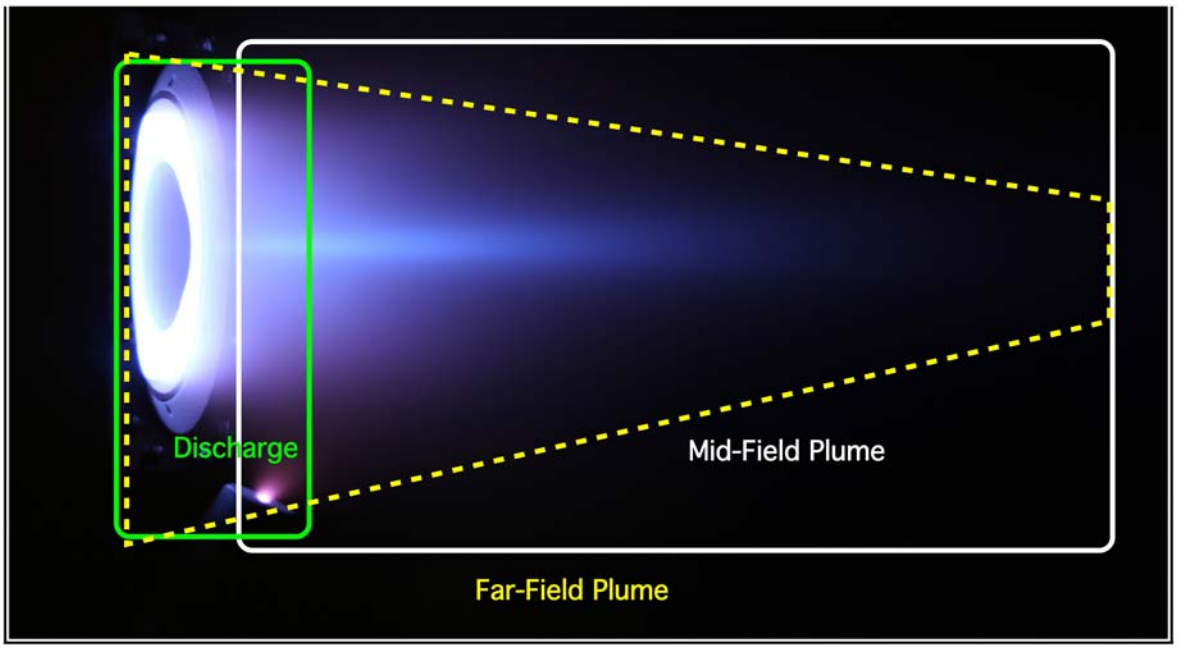

Fig. 12 Identified critical regions of Hall effect thruster discharge and plume.

core of the visible plume structure is composed of low velocity ions, some of which are streaming toward the central magnetic core. This central core is observed to extend further as the vacuum facility pressure is decreased. There are several critical processes believed to be occurring in this region, including cathode coupling and acceleration of divergent ions. At higher test pressures, it is believed that charge-exchange collisions produce large populations of slow moving ions and fast neutrals. At lower facility pressures it is believed that the number of charge-exchange collisions decreases, but the observed lengthening of the visible central core indicates that ion collisions or related transport processes continues, perhaps with reduced cross-field mobility. The mid–plume region of the Hall effect thruster discharge is important since it affects coupling of the cathode to the anode, has a relatively high density with observed collisional phenomena, and may produce ions damaging to a host spacecraft. As a result, the facility effects on the mid-plume are expected to propagate to both the thruster discharge and affect the development of the far–plume.

The far–plume we define as the region where collisions play a minimal role, at least in an operational orbital environment. It appears that adequately understanding this region is important since it is the region where designers would expect interactions with spacecraft to occur. Measurements of this region are presently suspect simply because the plasma must previously traverse the previous two other regions with obvious susceptibility to environmental facility conditions. As a result, accurate information in this region is dependent on understanding the effects in both the discharge and mid–plume regions of the discharge. Neither of which appears to be systematically available. In addition, how this region of the plasma interacts with the vacuum vessel has also not been addressed.

At the present state of technical understanding, the community has identified items of concern with respect to the test environments of Hall effect thruster ground test facilities. Systematic approaches appear to be lacking, as there has been a prevalent belief in the use of ad hoc corrections assuming that the ground test facility interactions only produce small changes in operating behavior. Previous work has shown that relatively small changes in the background pressure can produce fundamental changes in the anode discharge that then must by definition propagate downstream. This study has shown that prediction of these anode discharge behavior shifts appear to be dependent on thruster performance. Casual observations have also shown that the plume structure can change in consistent ways with background pressure, even if the mechanisms are not fully understood. We urge that coordinated research to adequately identify these critical interactions recognizing that distinct regions of the Hall effect plasma discharge are intrinsically linked be undertaken to produce a fundamental understanding so that the limitations of ground test for Hall effect thrusters can be adequately addressed.

Acknowledgments

This effort was funded by AFOSR with program monitor Dr. M. Birkan. The authors are also thankful for a number of fruitful discussions that enabled this paper as well as recent interest on the environmental conditions for Hall effect ground testing. Many col-

leagues have contributed in innumerable ways to this work. Early discussions with Drs. M. Fife and R. Spores provided the genesis for this effort. Discussions with Drs. D. Scharfe, M. Cappelli, and C. W. Larson created the interest in krypton propellant as a tool to understand the dynamics of Hall effect discharge physics. Dr. N. MacDonald–Tenenbaum served as a catalyst for the investigation through her thoughtful discussion of ionization fraction of the exit plane region of a Hall effect thruster. Many others have also contributed to the effort by way of their technical and material support. Ultimately, our result is *classically OCD!*

References

[1] M. R. Nakles and W. A. Hargus, "Background pressure effects on ion velocity distribution within a medium-power Hall thruster," *AIAA Journal of Propulsion and Power*, vol. 27, no. 4, pp. 737–743, July-August 2011.

[2] T. Randolph, V. Kim, H. Kaufman, K. Korzubusky, V. Zhurin, and M. Day, "Facility effects on stationary plasma thruster testing," in *Proceedings of the 23rd International Electric Propulsion Conference*, no. IEPC-1993-093. Seattle, WA: Electric Rocket Society, September 1993.

[3] D. R. Lide, *Handbook of Chemistry and Physics*, 79th ed. CRC Press, 1998.

[4] A. I. Bugrova, A. S. Lipatov, A. I. Morozov, and D. V. Churbanov, "On a similarity criterion for plasma accelerators of the stationary plasma type," *Technical Physics Letters (Trans. Pis'ma v Zhurnal Tekhinicheskoi Fizki)*, vol. 28, no. 10, pp. 821–823, 2002.

[5] J. A. Linnell and A. D. Gallimore, "Efficiency analysis of a Hall thruster operating with krypton and xenon," *Jounrnal of Propulsion and Power*, vol. 22, no. 6, pp. 1402–1418, November-December 2006.

[6] D. B. Scharfe, "Alternative hall thruster propellants krypton and bismuth: Simulated performance and characterization," Ph.D. dissertation, Stanford University, Palo Alto, CA, August 2009.

[7] A. I. Bugrova, A. M. Bishaev, A. V. Desyatskov, M. V. K. adn A. S. Lipatov, and M. Dudeck, "Experimental investigations of a krypton stationary plasma thruster," *International Journal of Aerospace Engineering*, vol. 2013, no. 686132, 2013.

[8] W. A. Hargus, G. M. Azarnia, and M. R. Nakles, "Kr II laser-induced fluorescence for measuring plasma acceleration," *Review of Scientific Instruments*, vol. 83, no. 103111, 2012.

[9] W. A. Hargus Jr. and M. A. Cappelli, "Laser-induced fluorescence measurements of velocity within a Hall discharge," *Applied Physics B*, vol. 72, no. 8, pp. 961–969, June 2001.

[10] W. A. Hargus and C. S. Charles, "Near exit plane velocity field of a 200 W Hall thruster," *Journal of Propulsion and Power*, vol. 24, no. 1, pp. 127–133, January-February 2008.

[11] S. Mazouffre, D. Gawron, V. Kulaev, and N. Sadeghi, "A laser spectroscopic study on Xe+ ion transport phenomena in a 5 kW-class Hall effect thruster," in *Proceedings of the 30th International Electric Propulsion Conference*, no. IEPC-2007-160. Florence, Italy: Electric Rocket Society, September 2007.

[12] M. R. Nakles and W. A. Hargus Jr., "Background pressure effects on internal and near-field ion velocity distribution of the BHT-600 Hall thruster," in *Proceedings of the 44th Joint Propulsion Conference and Exhibit*, no. AIAA-2008-5101. Hartford, CT: American Institute of Aeronautics and Astronautics, July 2008.

[13] W. A. Hargus Jr., M. R. Nakles, B. Pote, and R. Tedrake, "The effect of thruster oscillations on axial velocity distributions," in *Proceedings of the 44th Joint Propulsion Conference and Exhibit*, no. AIAA-2008-4724. Hartford, CT: American Institute of Aeronautics and Astronautics, July 2008.

[14] T. Fujimoto and A. Iwamae, Eds., *Plasma Polarization Spectroscopy*, ser. Series on Atomic, Optical and Plasma Physics. Springer-Verlag, 2008, vol. 44.

[15] W. A. Hargus, "A preliminary study of krypton laser-induced fluorescence," in *Proceedings of the 46th Joint Propulsion Conference and Exhibit*, no. AIAA-2010-6524. American Institute of Aeronautics and Astronautics, August 2010.

[16] W. A. Hargus, G. M. Azarnia, and M. R. Nakles, "Demonstration of laser-induced fluorescence on a krypton Hall effect thruster," in *Proceedings of the 32nd International Electric Propulsion Conference*, no. IEPC-2011-018. Electric Rocket Society, September 2011.

[17] G. Bourgeois, A. Lejune, and S. Mazouffre, "Ion velocity evolution with channel width, magnetic topology and propellant in a 200 W Hall thruster," in *Proceedings of the 32nd International Electric Propulsion Conference*, no. IEPC-2011-123. Electric Rocket Society, September 2011.

[18] M. R. Nakles, R. R. Barry, C. W. Larson, and W. A. Hargus, "A plume comparison of xenon and krypton propellant on a 600 W Hall thruster," in *Proceedings of the 31st International Electric Propulsion Conference*, no. IEPC-2009-118, Ann Arbor, MI, September 2009.

[19] I. Leybold-Heraeus Vacuum Proucts, *Vacuum Technology its Foundations Formulae and Tables*. Leybold-Heraeus Vacuum Proucts, Inc., 1987.

[20] W. A. Hargus and M. R. Nakles, "Ion velocity measurements within the acceleration channel of low-power Hall thruster," *IEEE Transactions on Plasma Science*, vol. 36, no. 5, pp. 1989–1997, October 2008.

[21] B. Barbieri, N. Beverini, and A. Sasso, "Optogalvanic spectroscopy," *Review of Modern Physics*, vol. 62, no. 3, pp. 603–644, July 1990.

[22] W. A. Hargus Jr. and M. R. Nakles, "Evolution of the ion velocity distribution in the near field of the BHT-200-x3 Hall thruster," in *Proceedings of the 42nd Joint Propulsion Conference and Exhibit*, no. AIAA-2006-4991. Sacramento, CA: American Institute of Aeronautics and Astronautics, July 2006.

[23] W. A. Hargus, G. M. Azarnia, and M. R. Nakles, "A comparison of ion acceleration characteristics for krypton and xenon propellants within a 600 watt Hall effect thruster," in *Proceedings of the 48th Joint Propulsion Conference and Exhibit*, no. AIAA-2012-3871. American Institute of Aeronautics and Astronautics, July-August 2012.

[24] J. M. Fife, "Hybrid-pic modeling and electrostatic probe survey of Hall thrusters," Ph.D. dissertation, Massachusetts Institute of Technology, Cambridge, MA, September 1998.

[25] E. Y. Choueiri, "Plasma oscillations in Hall thrusters," *Physics of Plasmas*, vol. 8, no. 4, pp. 1411–1426, April 2001.

[26] W. A. Hargus and M. A. Cappelli, "Interior and exterior laser-induced fluorescence and plasma measurements within a Hall thruster," *Jounrnal of Propulsion and Power*, vol. 18, no. 1, pp. 159–168, January-February 2002.

[27] W. A. Hargus Jr., "Laser-induced fluorescence measurements of neutral xenon in the near field of a 200 W Wall thruster," in *Proceedings of the 41st Joint Propulsion Conference and Exhibit*, no. AIAA-2005-4400. Tucson, AZ: American Institute of Aeronautics and Astronautics, July 2005.

[28] M. R. Nakles, L. Brieda, G. D. Reed, W. A. Hargus Jr., and R. L. Spicer, "Experimental and numerical examination of a Hall thruster plume," in *Proceedings of the 30th International Electric Propulsion Conference*, no. IEPC-2007-073. Florence, Italy: Electric Rocket Society, September 2007.

[29] M. R. Nakles, W. A. Hargus, J. J. Delgado, and R. L. Corey, "A performance comparison of xenon and krypton propellant on an SPT-100 Hall thruster," in *Proceedings of the 32nd International Electric Propulsion Conference*, no. IEPC-2011-003. Weisbaden, Germany: Electric Rocket Society, September 2011.

IEPC-2013-xxx

Background Pressure Effects on Krypton Hall Effect Thruster Internal Acceleration

William A. Hargus Jr.
Spacecraft Propulsion Branch, RQRS
Air Force Research Laboratory
Edwards Air Force Base, CA

Landon J. Tango
Michael R. Nakles
E.R.C., Inc.
Air Force Research Laboratory
Edwards Air Force Base, CA

Introduction

- **Why are we doing this work?**
  - **Continued examination of alternative Hall effect thruster propellants: Krypton**
  - **Interest in effects of test facility environments on Hall effect thruster operation**
  - **Fundamental differences attributable to propellant selection: Kr vs Xe**
- **Why use laser induced Kr II fluorescence (LIF)?**
  - **Non-intrusive measurements via LIF producing ion acceleration profiles and velocity distributions**
  - **Low mass of Kr will increase diffusion from facility into discharge (~25% increase; 84 amu vs 131 amu Xe)**
- **What information do we hope to extract?**
  - **Continued optimization of Kr in a Hall effect thruster**
  - **Changes in thruster operation due to Kr ingestion relative to Xe**

Photograph of BHT-600 operating on krypton

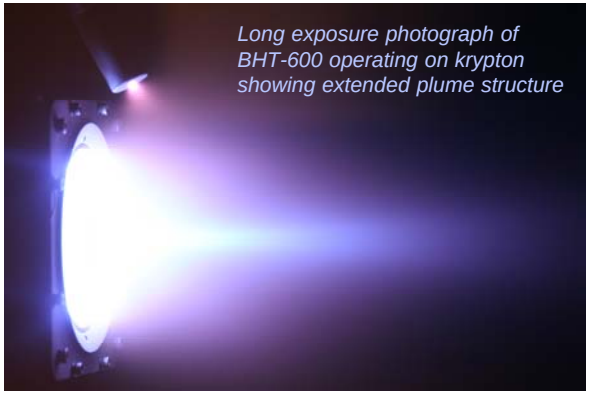

Long exposure photograph of BHT-600 operating on krypton showing extended plume structure

Krypton for Electrostatic Thrusters

Comparison of Xenon to Krypton Properties

Property	Units	Xe	Kr
Atomic Mass	amu	131.3	83.8
1^{st} Ionization Energy	eV	12.1	14.0
2^{nd} Ionization Energy	eV	21	24
3^{rd} Ionization Energy	eV	32	37
Atmospheric Concentration	ppb	87	1000
Stable Isotopes		9	6
Odd Isotopes		2	1
Critical Pressure	MPa	5.84	5.50
Critical Temperature	K	290	209
Boiling Point (1 atm)	K	161	120

Krypton Similar to Xenon

- Noble gases, not widely separated
- Physical properties are similar
- Electrons bound more tightly
  - Less electron shielding
  - Higher ionization energies, +15%
- More ideal gas behavior
  - Less compressible
  - More difficult pressurized storage

Krypton vs Condensibles

- Kr is nearly Xe "drop in" replacement
  - No changes required to thruster
  - Minimal changes required to propellant management
  - No increased likelihood of S/C contamination
- Compare to Bismuth…
  - Thruster design modifications
  - High temperature propellant distribution
  - Significant likelihood of S/C contamination

Busek BHT-600

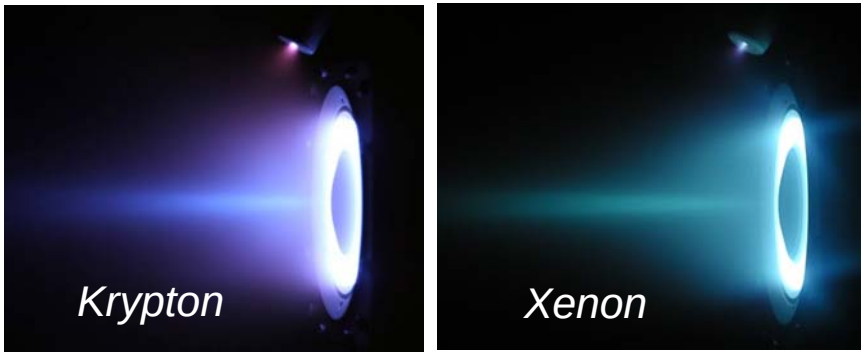

IEPC-2009-115, Nakles et al.

Medium Power Hall Effect Thruster and Test Facility

AFRL Chamber 6, Edwards AFB

- Cryogenic pumping
  - 5 independent pumps
  - 32,000 l/s
- Stainless Steel chamber walls
  - 1.8 m diameter, 3.0 m length
  - Graphite beam dump

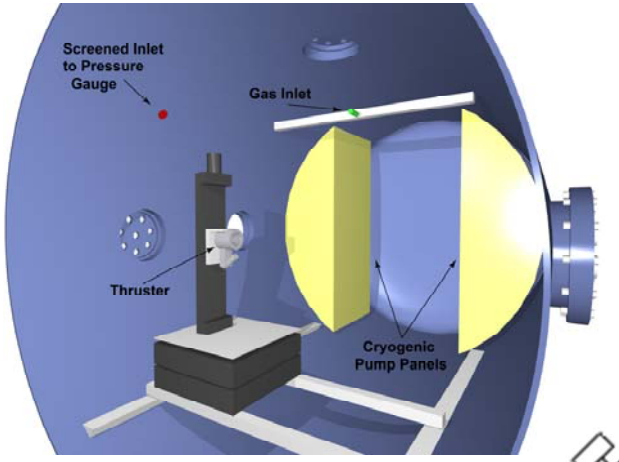

BUSEK

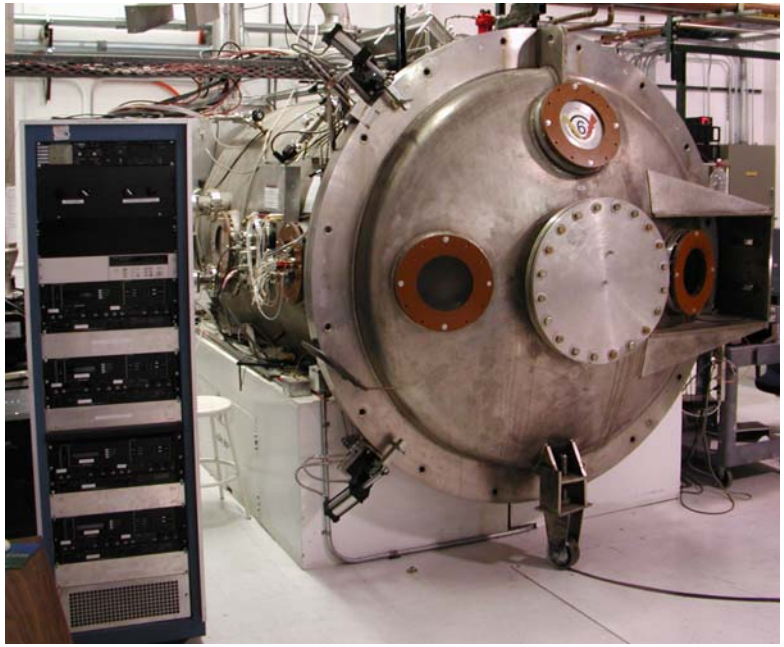

Minimum Pressure: 1.2x10^{-5} Torr
Maximum Pressure: 3.2x10^{-5} Torr

Both pressures are below accepted 5x10^{-5} Torr upper limited for long duration HET testing

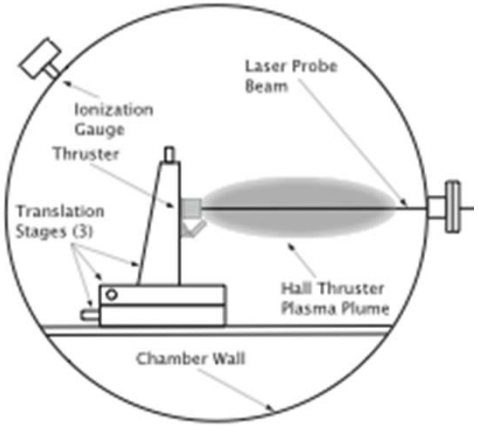

Medium Power Laboratory HET

- Busek BHT-600 operating at 600 W
- Single operating condition examined
- Previously measured xenon acceleration
- Performance characterized

Comparison of Global Parameters

Krypton Operating Parameters

Kr Anode Flow	25.5 sccm (1.59 mg/s)
Kr Cathode Flow	1.5 sccm (94 μg/s)
Anode Potential	300 V
Anode Current	1.73 A
Inner Coil Current	1.75 A
Outer Coil Current	1.75 A
Keeper Current	0.5 A
Heater Current	3.0 A
Thrust	22.4 mN
Anode Efficiency	31%
Specific Impulse	1440 s

Thrust measurements from Nakles, Larson, and Hargus, IEPC-2009-118

Xenon Operating Parameters

Xe Anode Flow	25.5 sccm (2.5 mg/s)
Xe Cathode Flow	1.5 sccm (147 μg/s)
Anode Potential	300 V
Anode Current	1.93 A
Inner Coil Current	1.75 A
Outer Coil Current	1.75 A
Keeper Current	0.5 A
Heater Current	3.0 A
Thrust	35.8 mN
Anode Efficiency	44%
Specific Impulse	1460 s

Xenon LIF measurements from Nakles and Hargus, JPP, vol. 27, no. 4, 2011.

Laser-Induced Fluorescence Apparatus and Regions of Detailed Examination

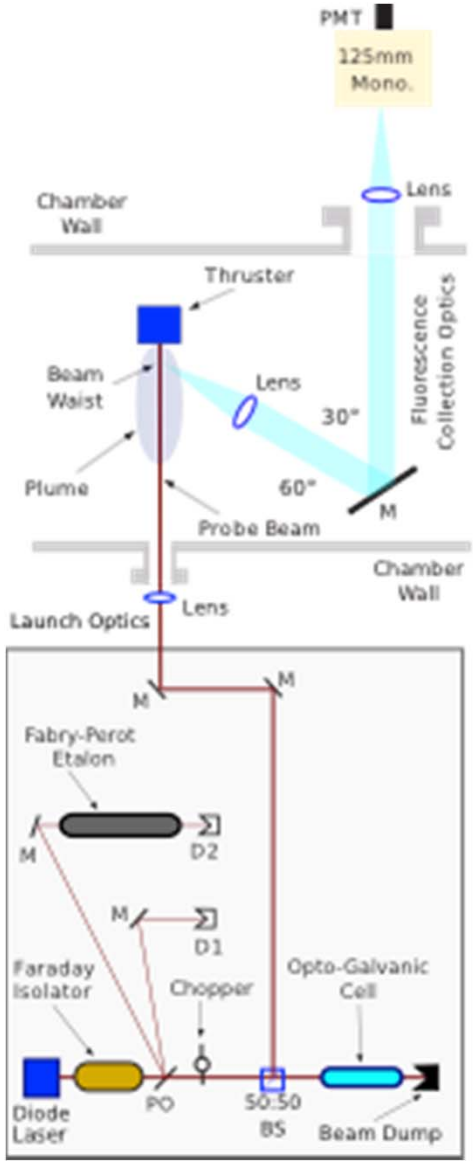

- **Single axis LIF with interior optical axis into thruster**
  - Similar to previous LIF apparatus (Hargus & Nakles, IEEE Plas Trans 2008)
- **Single region of detailed examination**
  - Centerline of acceleration channel
  - Good measurement of…
    - Energy deposition (acceleration, implied electric fields)
    - Ionization processes (regions of ion creation)
  - Compare to historical xenon data
    - Same thruster!
    - Same applied acceleration potential
    - Same magnetic field
  - Result: Very different plasma…

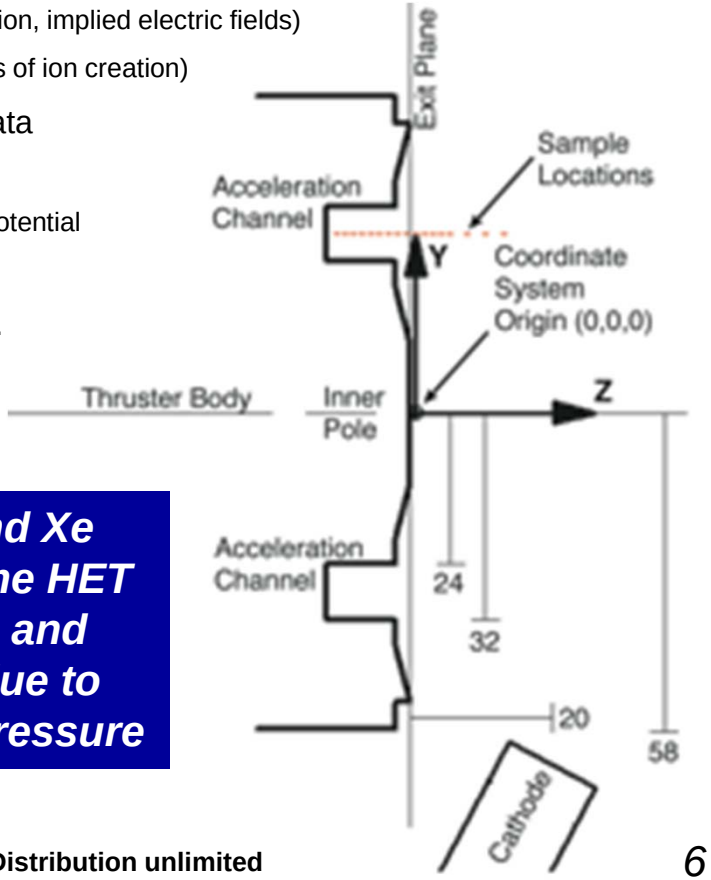

Goal: Compare Kr and Xe acceleration in the same HET at similar conditions and identify differences due to elevated background pressure

General Trends of Krypton Operation (Low Facility Pressure)

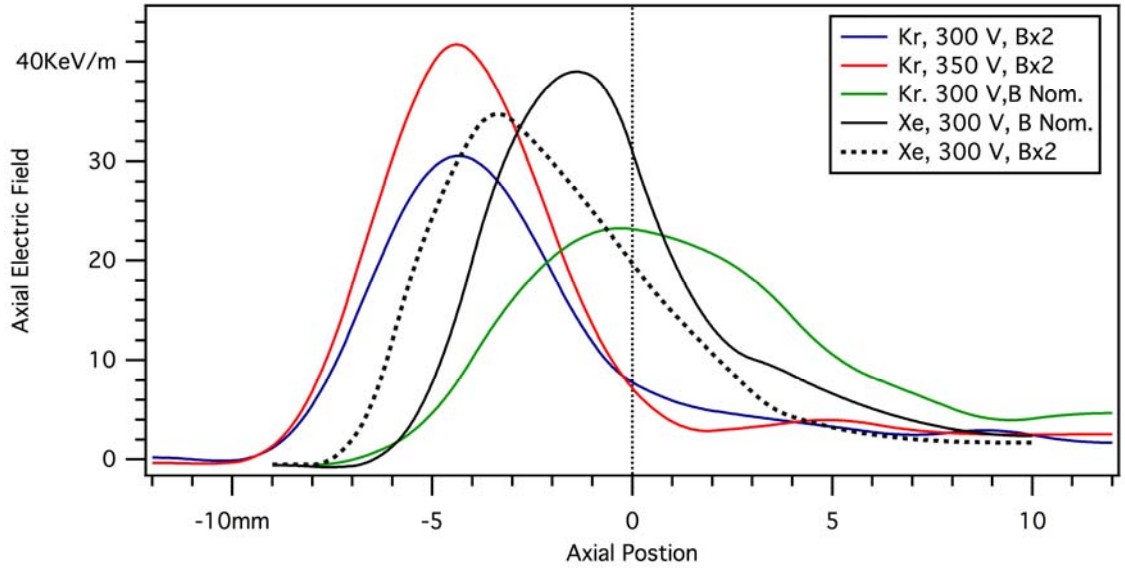

- **Xenon and krypton operation initially show very different electric fields**
  - Xenon (black) shows a higher field, peaking within thruster channel
  - Krypton (green) exhibits a lower, broader E field, peaking at the exit plane
- **Response to thruster input variables (e.g. B field, applied discharge potential) is similar**
  - Raising B field pushes peak field toward anode
  - Electric field profile of krypton approaches that of xenon at increased potential and B field
  - Increasing discharge potential increases the electric field
- **Electric field profile of krypton approaches that of xenon at increased potential and B field**
  - While krypton operation is not optimized, it appears similar to that of xenon with respect to ion acceleration!

Krypton Most Probable Ion Velocities at Low and High Facility Pressures

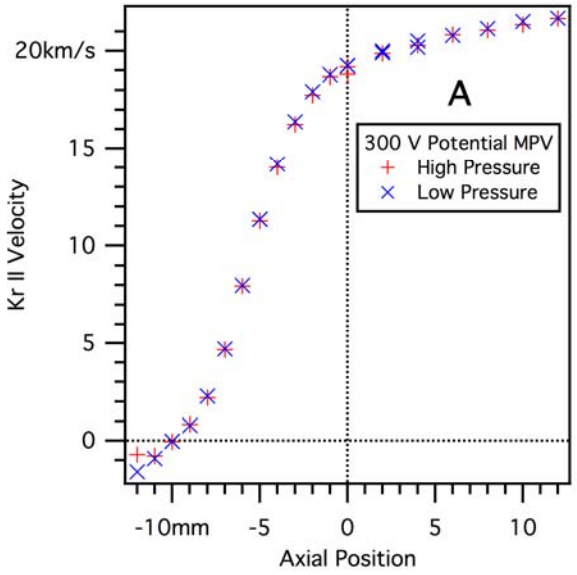

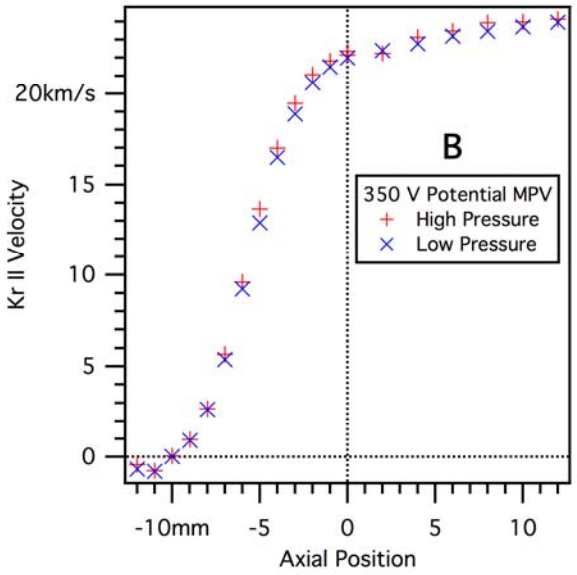

- **Most Probable Velocity (MPV) of the ions**
  - Peak of velocity distribution
  - Simple metric with low ambiguity, readily identifiable even with noisy data
  - Used to produce E fields in previous chart
- **Low and High facility pressure operation**
  - Low pressure case of minimum facility pressure 1.2E-5 Torr (Kr corrected)
  - High pressure case with 40 sccm Kr injection at 3.2E-5 Torr (Kr corrected)
  - Previous study showed dramatic difference in internal ion acceleration (Ref. 1)
- **Krypton 300 V case (low vs high pressure)**
  - Virtually no difference in MPV
  - Velocity distributions did broaden some, but peaks unchanged (next page)
- **Krypton 350 V case (low vs high pressure)**
  - MPV increased slightly, as much as 1 km/s
  - Velocity distributions also broadened, but less so than 300 V case
- **Unexpectedly krypton operation does not produce the substantial changes shown by xenon for the same conditions**

Krypton Ion Velocity Distributions at Low and High Facility Pressures

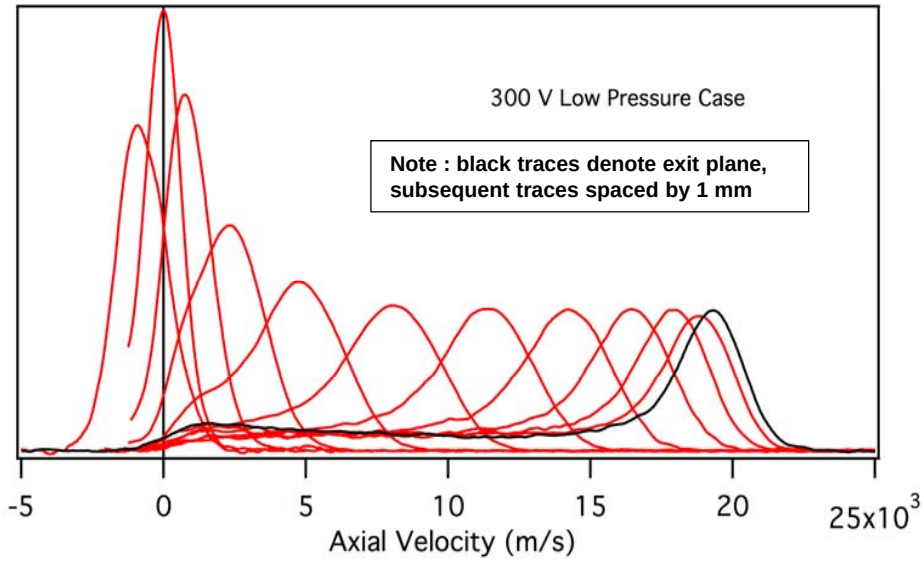

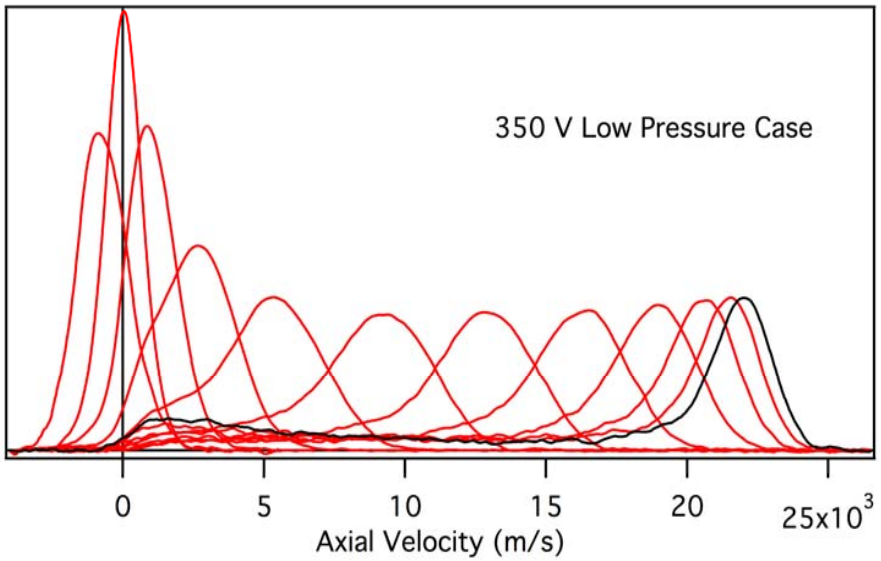

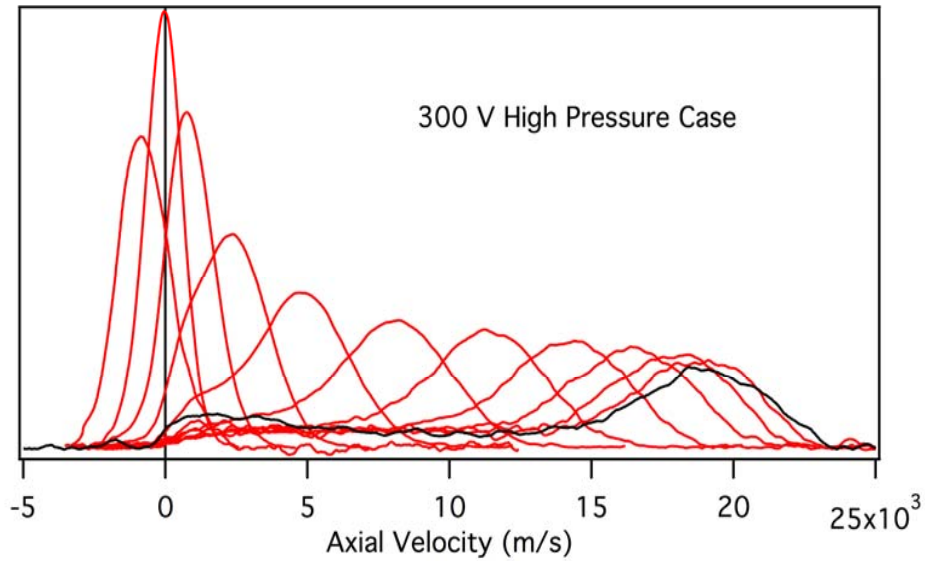

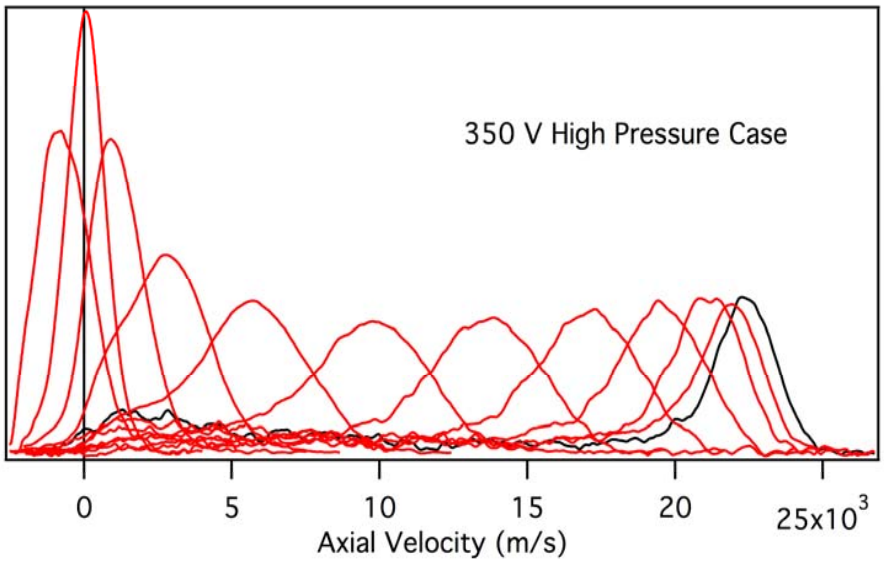

Kr Integrated Populations within Thruster Channel

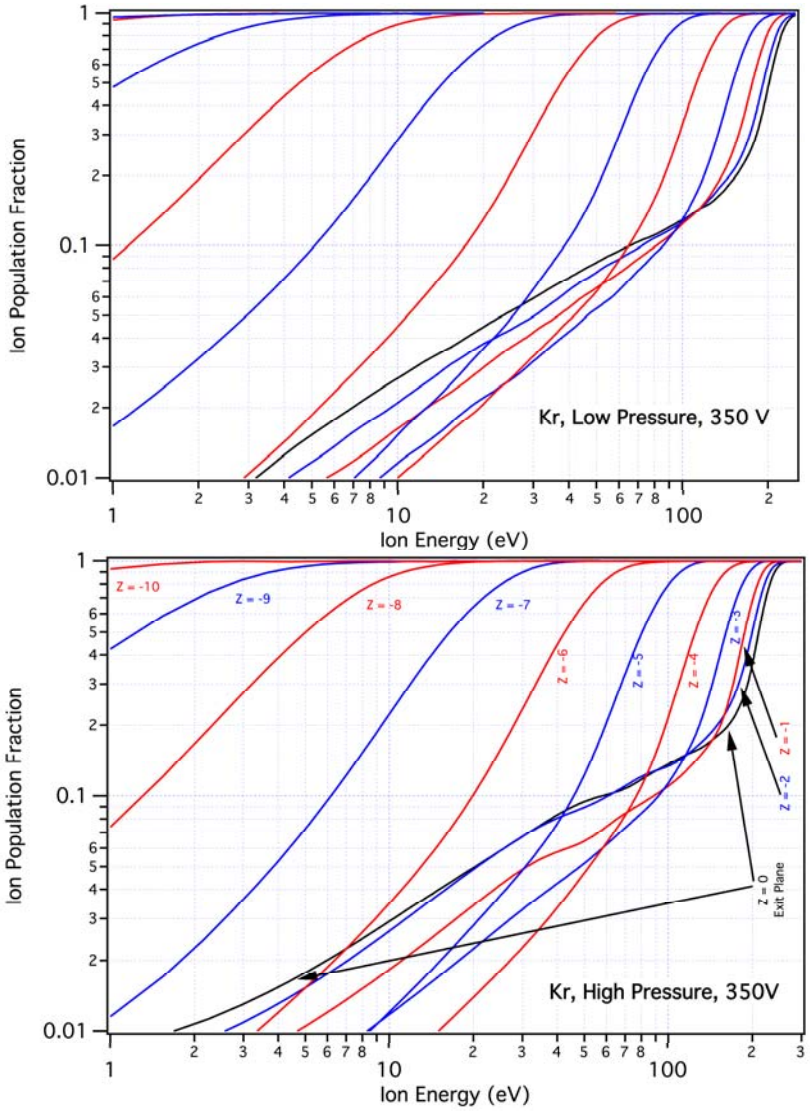

- **Integrated ion energy populations**
  - Converted VDFs to energy distributions (1/2 mv^2)
  - Running integration between 0 and 1 (100%)
- **Ion acceleration and late term ionization**
  - Late term ionization prevalent due to low propellant utilization
  - Ionization creates low energy ion populations
  - Monotonic spacing of lines expected if ionization rate remains constant
  - Crossing of positional integrations indicates substantial increases of ionization near exit plane (both cases)
- **Differences between low and high pressure cases**
  - Increase of 50% low energy ions, apparently locally ionized
  - Likely evidence of ingestion
  - Subtle differences
  - Only at population fractions less than 0.2 diverge
  - Similar general behavior

Kr Integrated Populations within Thruster Channel (Ref #1)

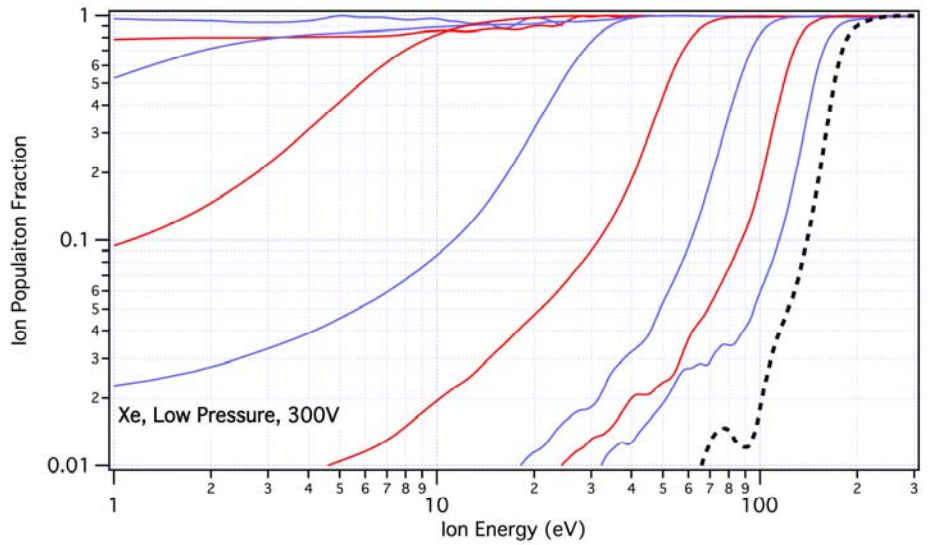

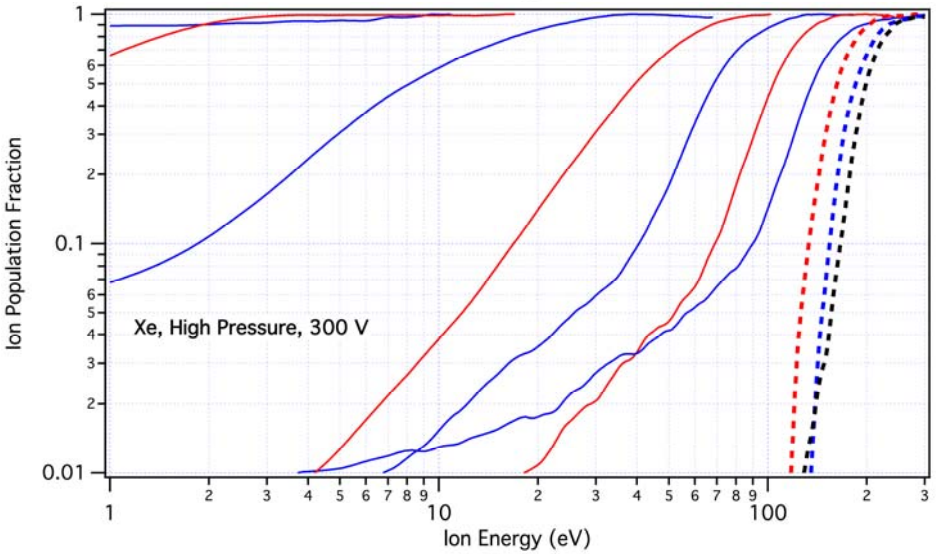

- **Integrated ion energy populations for xenon**
  - Taken from Ref # 1
  - Same flow and thruster inputs, similar back pressures
  - 3x lower integration time degrades SNR ~2x
    - Data below ~0.03 population faction questionable
  - Xe data substantially noisier near exit plane
    - Dashed lines for LARGE uncertainty below 0.1 population fraction
    - Especially in high pressure case
- **Effects of elevated pressure for xenon**
  - Xe cases appear to only show overlapping integration curves for high pressure case
  - Limited basis of comparison due to low SNR
- **Comparison to krypton case**
  - Xenon shows less population overlap, less ingestion
  - Xenon shows overlap for only high pressure case
  - SNR precludes definitive connection, but provides corroborating evidence that ingestion is affecting the ion population and energy distribution

Magnitudes of Exit Plane Densities for BHT-600 Thruster (Kr & Xe)

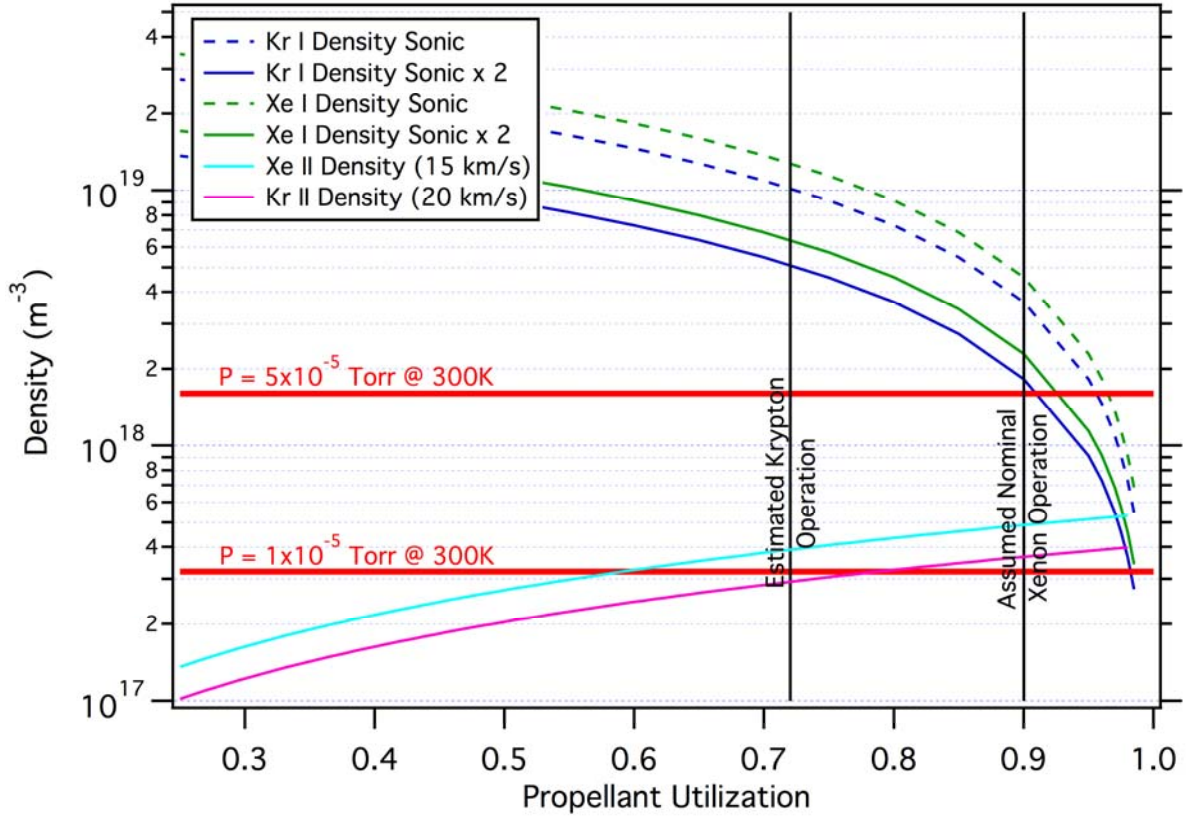

What are the relative densities of the neutrals and ions exiting the thruster and the background facility density?

Exiting neutral density calculated from Xe neutral velocity measurements, approximated by 2x room temperature sonic velocity, and propellant utilization fraction

Exiting ion density calculated from Xe & Kr ion velocity , and propellant utilization fraction

Facility density calculated as ideal gas at 300 K. Note, cryogenic systems may reduce temperature and facility densities may be substantially higher

Performance measurements of krypton imply propellant utilization of 0.8x that of xenon (taken to be 0.9), yielding krypton propellant utilization of ~0.72

- **Krypton cases – facility pressure has no substantial effect**
  - Exit neutral density >> facility neutral density (both cases)
- **Xenon cases – facility pressure has substantial effect**
  - High pressure case: exit neutral density ~ facility neutral density
  - Low pressure case: exit neutral density >> facility neutral density

Relative density of neutrals at exit plane (thruster vs environment) appears to produce substantial changes in discharge dynamics

Summary and Conclusions and Future Work

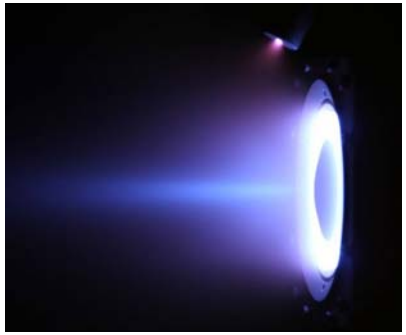

- **Krypton thruster operation responds to control variables similarly to xenon**
  - Raising the magnetic field, moves acceleration toward anode
  - Increased facility pressure moves acceleration toward anode
- **Krypton shows substantially less susceptibility to facility neutral pressure**
  - Xenon interior acceleration changes with facility pressure dramatically
  - Krypton interior acceleration shows only small changes in shape of velocity distribution
- **Neutral densities exiting thruster and of facility appear to be critical**
  - Krypton operation has substantially lower propellant utilization (0.7), hence density of neutrals exiting thruster remain far above facility background
  - Xenon operation has good propellant utilization (0.9), hence density of neutrals exiting thruster approach that of high facility pressure case
  - Low facility pressure case has neutral densities approximately that of ion densities exiting thruster; suggests facility pressure remains above optimal
- **Future Work: see next page**
  - Need to understand the dynamics within the critical regions of a Hall effect thruster discharge and plume…

Critical Regions of a Hall Effect Thruster Discharge and Plume

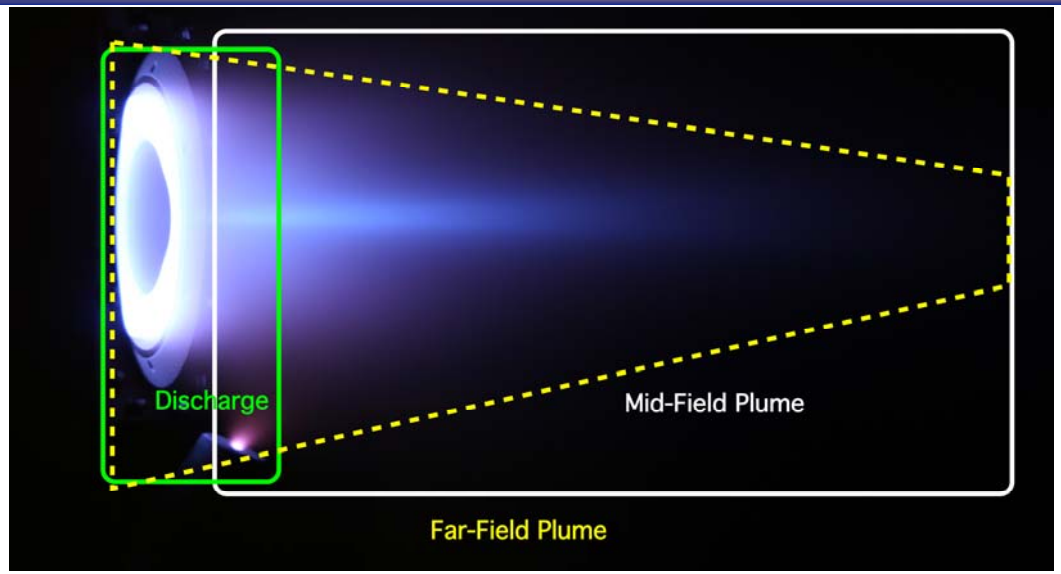

Much prior work has examined one of more aspects of facility effects on Hall effect thruster testing, most focused on empirical mitigation of effects

Systematic studies of the effects of ground test facilities on each of these regions is necessary

- **Division of Hall effect plasma into three overlapping regions**
- **Discharge (within green box)**
  - Region of ionization and acceleration of propellant
  - Ranges from the anode to vicinity of cathode
- **Mid-Plume (within white box)**
  - Luminous, collisional region outside thruster body, includes near-plume external acceleration
  - Region with isolated slow ion population in central core and responsible for cathode coupling
- **Far-Plume (outside yellow trapezoid)**
  - Region of low collisional probability, far from thruster and influence of applied fields
  - Region of interest to spacecraft integrators and dependant on behavior of both prior regions